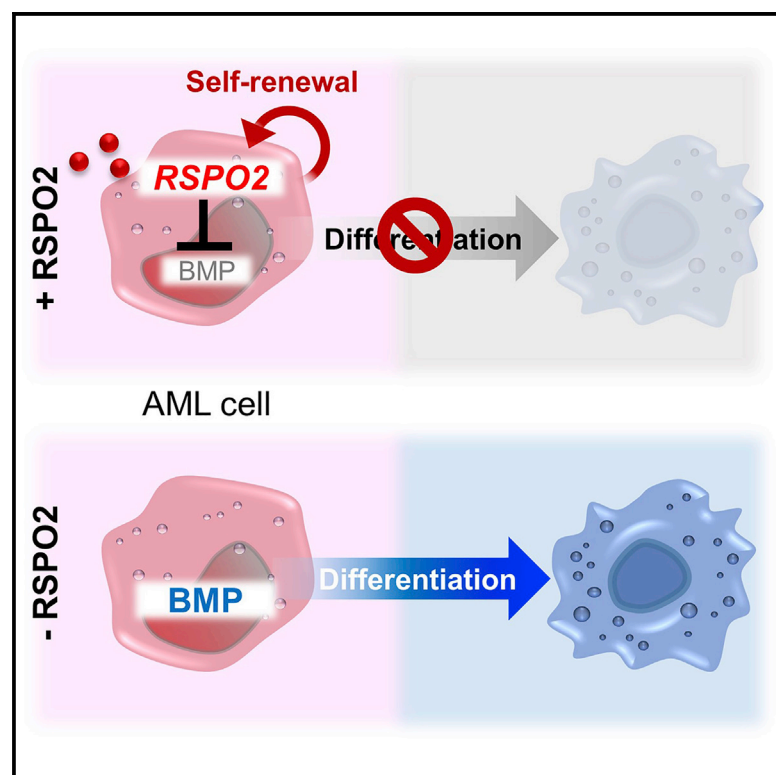


Cell Reports

RSPO2 inhibits BMP signaling to promote self-renewal in acute myeloid leukemia

Graphical abstract



Authors

Rui Sun, Lixiazi He, Hyeyoon Lee, ..., Karin Müller-Decker, Caroline Pabst, Christof Niehrs

Correspondence

niehrs@dkfz-heidelberg.de

In brief

Sun et al. report that the secreted stem cell growth factor R-spondin 2 (RSPO2) acts as a BMP signaling antagonist to promote self-renewal in acute myeloid leukemia cells. High *RSPO2* expression predicts poor prognosis, suggesting RSPO2 as potential prognostic marker and drug target in AML.

Highlights

- RSPO2 is a regulator of AML cell self-renewal
- RSPO2 acts as a BMP antagonist instead of as a WNT agonist in AML
- High *RSPO2* expression is a marker for adverse prognosis in AML



Sun et al., 2021, Cell Reports 36, 109559
August 17, 2021 © 2021 The Author(s).
<https://doi.org/10.1016/j.celrep.2021.109559>

Article

RSPO2 inhibits BMP signaling to promote self-renewal in acute myeloid leukemia

Rui Sun,¹ Lixiazi He,^{2,3} Hyeyoon Lee,¹ Andrey Glinka,¹ Carolin Andresen,^{4,5} Daniel Hübschmann,^{5,6} Irmela Jeremias,^{7,8} Karin Müller-Decker,⁹ Caroline Pabst,^{2,3} and Christof Niehrs^{1,10,11,*}

¹Division of Molecular Embryology, DKFZ-ZMBH Alliance, Deutsches Krebsforschungszentrum (DKFZ), 69120 Heidelberg, Germany

²Department of Medicine V, Hematology, Oncology and Rheumatology, University of Heidelberg, 69120 Heidelberg, Germany

³Molecular Medicine Partnership Unit, European Molecular Biology Laboratory–Heidelberg University Hospital, 69120 Heidelberg, Germany

⁴Division of Stem Cells and Cancer, Deutsches Krebsforschungszentrum (DKFZ) and DKFZ-ZMBH Alliance, 69120 Heidelberg, Germany

⁵Heidelberg Institute for Stem Cell Technology and Experimental Medicine (HI-STEM), 69120 Heidelberg, Germany

⁶Computational Oncology, Molecular Diagnostics Program, National Center for Tumor Diseases (NCT) Heidelberg and DKFZ, 69120 Heidelberg, Germany

⁷Research Unit Apoptosis in Hematopoietic Stem Cells, Helmholtz Zentrum München, German Research Center for Environmental Health (HMGU), Munich, Germany

⁸German Cancer Consortium (DKTK), partner site Munich, Germany

⁹Core Facility Tumor Models, Deutsches Krebsforschungszentrum (DKFZ), 69120 Heidelberg, Germany

¹⁰Institute of Molecular Biology (IMB), 55128 Mainz, Germany

¹¹Lead contact

*Correspondence: niehrs@dkfz-heidelberg.de

<https://doi.org/10.1016/j.celrep.2021.109559>

SUMMARY

Acute myeloid leukemia (AML) is a rapidly progressing cancer, for which chemotherapy remains standard treatment and additional therapeutic targets are requisite. Here, we show that AML cells secrete the stem cell growth factor R-spondin 2 (RSPO2) to promote their self-renewal and prevent cell differentiation. Although RSPO2 is a well-known WNT agonist, we reveal that it maintains AML self-renewal WNT independently, by inhibiting BMP receptor signaling. Autocrine RSPO2 signaling is also required to prevent differentiation and to promote self-renewal in normal hematopoietic stem cells as well as primary AML cells. Comprehensive datamining reveals that RSPO2 expression is elevated in patients with AML of poor prognosis. Consistently, inhibiting RSPO2 prolongs survival in AML mouse xenograft models. Our study indicates that in AML, RSPO2 acts as an autocrine BMP antagonist to promote cancer cell renewal and may serve as a marker for poor prognosis.

INTRODUCTION

Acute myeloid leukemia (AML) is an aggressive hematological cancer characterized by uncontrolled proliferation of hematopoietic stem/progenitor cells (HSPCs) and blockage of myeloid differentiation (De Kouchkovsky and Abdul-Hay, 2016; Döhner et al., 2015; Nowak et al., 2009). Owing to its highly heterogeneous genetic background, treatment of AML is inherently complex with poor and variable success rates (Balgobind et al., 2011; Ivey et al., 2016; Li et al., 2016). Thus, comprehensive understanding of the mechanisms governing the proliferation and differentiation of AML cells is required for biomarker development, precise risk stratification, and, eventually, configuration of personalized treatments. Leukemia is initiated and maintained by self-renewing leukemia stem cells (LSCs) that share properties with hematopoietic stem cells producing normal blood cells (Gal et al., 2006). Identification of signaling pathways regulating LSCs' self-renewal is of great interest, as targeting these signals could offer therapeutic benefit.

WNT and BMP signaling pathways are implicated in aberrant AML cell proliferation during disease progression (Gruber

et al., 2012; Imai et al., 2001; Jiang et al., 2000; Majeti et al., 2009; Raymond et al., 2014; Topić et al., 2013; Voeltzel et al., 2018; Wang et al., 2006, 2010; Yeung et al., 2010). For instance, β -catenin, the transcriptional co-activator and downstream mediator of the canonical WNT pathway, is activated in developing leukemia cells and is required for the transformation of committed myeloid progenitors (Wang et al., 2010). Conversely, genetic ablation of β -catenin abolishes the oncogenic potential of leukemia cells (Yeung et al., 2010). Regarding BMP signaling, some studies have demonstrated that activation of the pathway maintains progenitors in an undifferentiated state, resulting in therapeutic resistance (Gruber et al., 2012; Raymond et al., 2014; Topić et al., 2013; Voeltzel et al., 2018), while others reported that BMP signaling inhibits growth and induces differentiation of myeloid progenitors and AML cells (Imai et al., 2001; Jiang et al., 2000; Wang et al., 2006).

R-spondins (RSPO1–RSPO4) are secreted stem cell growth factors implicated in development, stem cell maintenance, and cancer (Chartier et al., 2016; de Lau et al., 2014; Hao et al., 2016; Kazanskaya et al., 2004; Kim et al., 2005; Nanki et al., 2018; Seshagiri et al., 2012). As potent WNT signaling agonists,



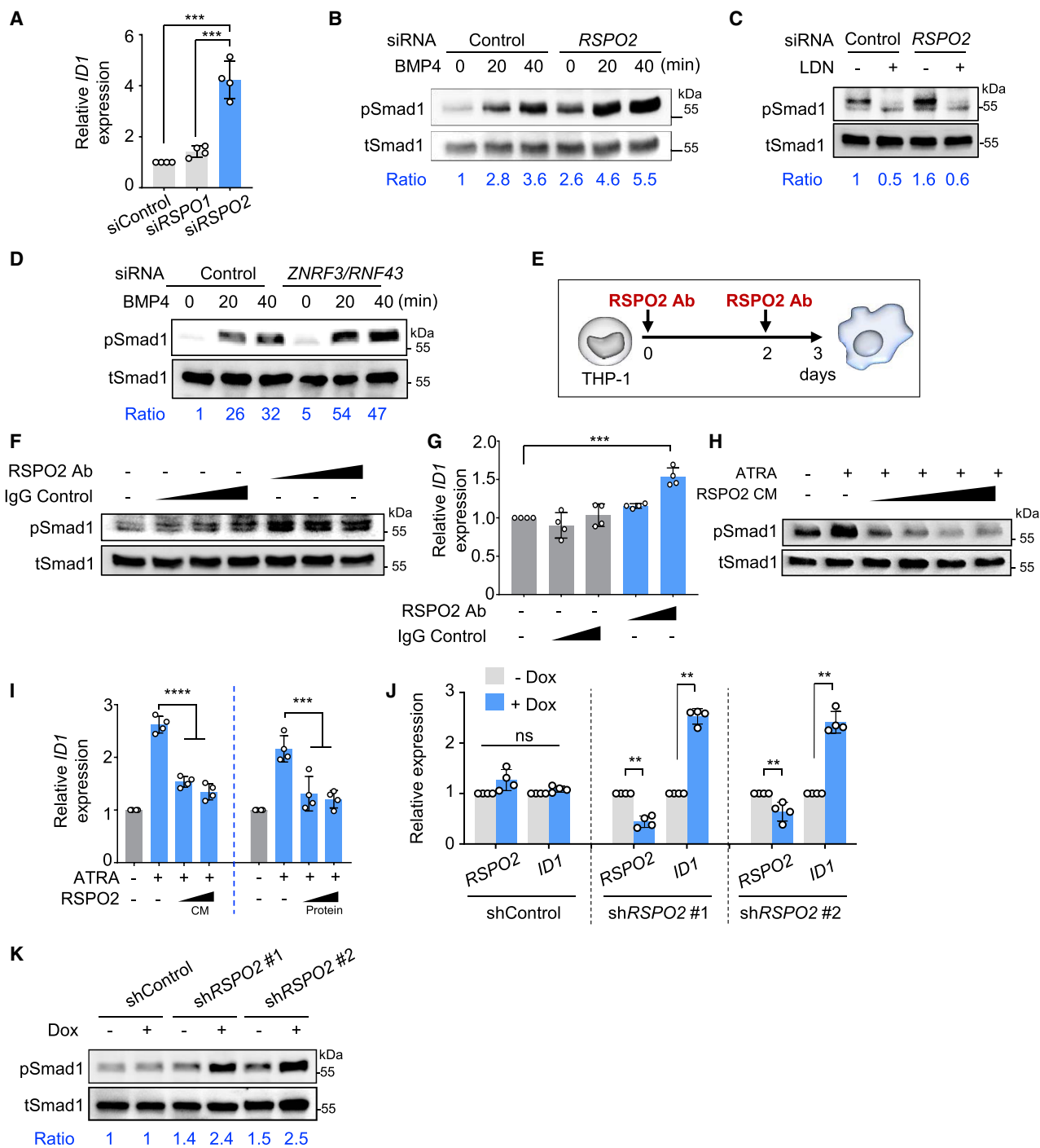


Figure 1. RSP02 antagonizes BMP signaling in AML cells

(A) qRT-PCR analysis of the BMP target gene *ID1* in THP-1 cells transfected with siRNAs as indicated. n = 4 per group.
 (B) Western blot analysis of phosphorylated (p)Smad1 and total (t)Smad1 in THP-1 cells treated with siRNA and BMP4 as indicated. After overnight starvation, cells were stimulated with 5 ng/ml BMP4 for 20 and 40 min. Ratio shows relative levels of pSmad1 normalized to tSmad1.
 (C) Western blot analysis of pSmad1 and tSmad1 in siRNA-treated THP-1 cells, with or without BMP receptor inhibitor (LDN-193189, LDN) treatment. Cells were treated with 300 nM LDN overnight before analysis. Ratio shows relative levels of pSmad1 normalized to tSmad1.
 (D) Western blot analyses of pSmad1 and tSmad1 in THP-1 cells treated with siRNA and BMP4 as indicated. After overnight starvation, cells were stimulated with 5 ng/ml BMP4 for 20 and 40 min. Ratio shows relative levels of pSmad1 normalized to tSmad1.
 (E) Experimental scheme of RSP02 neutralization assay. Ab, antibody.

(legend continued on next page)

RSPOs promote the specification and development of hematopoietic lineages (Genthe and Clements, 2017; Salik et al., 2020; Wang et al., 2019). Mechanistically, RSPOs amplify WNT signaling by binding to leucine-rich repeat containing G protein-coupled receptors 4–6 (LGR4–LGR6) and sequestering ring finger 43 (RNF43) and zinc and ring finger 3 (ZNR3). RNF43 and ZNR3 are E3 ubiquitin ligases that ubiquitinate and target the Frizzled/LRP5/6 WNT receptors for degradation (Carmon et al., 2011; Glinka et al., 2011; Hao et al., 2012, 2016; Koo et al., 2012). In AML, RSPO3–LGR4 signaling is essential for stem cell proliferation (Salik et al., 2020).

Supplementing the long-held view that RSPOs function exclusively through the WNT pathway, we recently reported a role for RSPO2 and RSPO3 as BMP signaling antagonists (Lee et al., 2020). BMPs signal through a tetrameric receptor kinase complex composed of type I and type II receptors (Heldin and Moustakas, 2016). Ligands and receptors interact in a combinatorial fashion (Antebi et al., 2017) and phosphorylate SMAD1, SMAD5, and SMAD8, which enter the nucleus with SMAD4 to regulate target gene expression (Heldin et al., 1997; Massagué, 1998). There exists a multitude of extracellular modulators of transforming growth factor (TGF)- β signaling, either soluble or membrane-associated proteins that control ligand availability, processing, ligand-receptor interaction, and receptor activation (Chang, 2016). In this context, we show that RSPO2 acts as a BMP antagonist independent of LGRs and WNT receptors: RSPO2 binds the BMP receptor ALK3/BMPRI1 and engages ZNR3 to trigger internalization and degradation of ALK3 (Lee et al., 2020). Hence, certain RSPOs are bifunctional ligands, which activate WNT and inhibit BMP signaling. *In vivo* support for this RSPO2 function comes from early *Xenopus* embryos, where RSPO2 cooperates with Spemann organizer effectors to inhibit BMP signaling during axis formation (Lee et al., 2020).

RSPO2 and RSPO3 are involved in tumorigenesis (Hao et al., 2016), raising the question of whether BMP inhibition by RSPOs may also be relevant in disease. Here, we show that BMP inhibition by RSPO2 plays a role in maintaining autocrine self-renewal in AML cell lines and primary patient-derived xenograft (PDX)-derived AML cells (i.e., it promotes AML cell proliferation and impairs differentiation by inhibiting BMP receptor signaling). In patients with AML, elevated RSPO2 expression is highly predictive of poor prognosis. Consistently, inhibition of RSPO2 in xenografted AML mouse models reduces disease progression. Our study recommends RSPO2, a druggable secreted protein, as a candidate prognostic marker and therapeutic target in AML.

RESULTS

RSPO2 antagonizes BMP signaling in AML cells

We were intrigued by the observation that in coexpression data-mining with Coexpedia (Yang et al., 2017), the top “Medical Subject Heading” hit for *Rspo2* was “Macrophages,” a cell type whose maturation from precursors (monocytes) is regulated by BMP signaling (Pardali et al., 2018; Rocher et al., 2012). Since RSPO2 is also a BMP signaling inhibitor, we investigated its role in the context of human monocytic leukemia and employed THP-1 cells, which displayed the highest RSPO2 expression among various tested AML cell lines (Figures S1A and S1B). THP-1 cells are used to model both monocyte-to-macrophage differentiation and AML (Auwerx, 1991). THP-1 cells are derived from a patient with monocytic leukemia (AMoL, or AML-M5), carrying t(9;11)(p22;q23) and expressing MLL-AF9 fusion protein. They can be maintained in culture to undergo self-renewing cell divisions or can be induced to differentiate into macrophages.

Consistent with our observations in human cell lines and *Xenopus* (Lee et al., 2020), RSPO2, but not RSPO1, small interfering RNA (siRNA) knockdown in THP-1 cells enhanced BMP signaling, as shown by induction of *ID1* expression (Figure 1A). Furthermore, RSPO2 knockdown was accompanied by increased Smad1-phosphorylation (Figure 1B), and treatment with the BMP receptor inhibitor LDN 193189 (Cuny et al., 2008) reverted this induction (Figure 1C). Likewise, siZNR3/RNF43 enhanced Smad1-phosphorylation (Figure 1D). In contrast, while reducing cytosolic β -catenin protein levels, siLGR4 had no effect on Smad1-phosphorylation (Figures S1C and S1D). Similarly, siLRP5/6 did not increase *ID1* expression (Figure S1E). To confirm the effect of siRSPO2, we employed a neutralizing anti-RSPO2 antibody (Ab), which inhibited the WNT reporter (TOPflash) activity induced by recombinant RSPO2 in HEK293T cells and decreased cytosolic β -catenin levels in THP-1 cells (Figures S1F and S1G). Similar to siRSPO2 treatment, neutralizing endogenous RSPO2 protein with the anti-RSPO2 Ab increased Smad1-phosphorylation and *ID1* expression (Figures 1E–1G).

To test the effects of RSPO2 treatment, we incubated THP-1 cells with RSPO2 recombinant protein, which increased cytosolic β -catenin levels (Figure S1H). By contrast, RSPO2 decreased BMP signaling activity induced by BMP4 or siRSPO2 (Figures S1I–S1K). In addition, we stimulated THP-1 cells with all-*trans*-retinoic acid (ATRA), which regulates BMP signaling in multiple contexts (Cruz et al., 2019; Shao et al., 2016). ATRA administration induced Smad1-phosphorylation and *ID1*

(F) Western blot analysis in THP-1 cells treated with neutralizing Ab as indicated. The 0.3, 1.0, and 3.0 μ g/ml Abs were used for the experiment.

(G) qRT-PCR analysis of *ID1* in THP-1 cells treated with neutralizing Ab as indicated. The 1.0 and 3.0 μ g/ml Abs were used for the experiment. $n = 4$ per group.

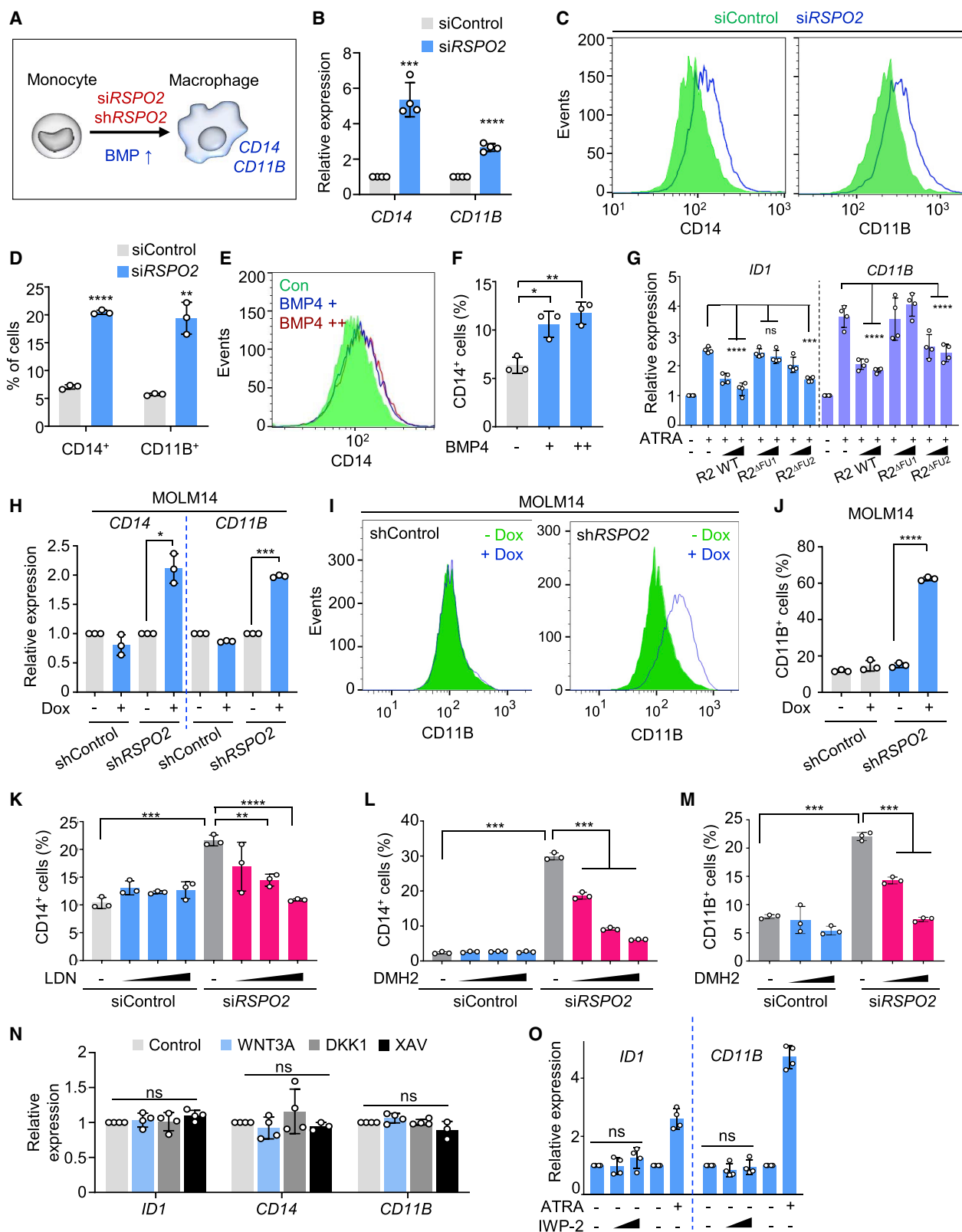
(H) Western blot analysis of pSmad1 and tSmad1 in THP-1 cells stimulated by 10 nM ATRA, with or without increasing amounts of RSPO2-CM for 3 days. ATRA, all-*trans*-retinoic acid; CM, conditioned medium.

(I) qRT-PCR analysis of *ID1* in THP-1 cells stimulated by 10 nM ATRA, with or without increasing amount of RSPO2 recombinant protein (0.2 and 0.5 μ g/ml) and CM for 3 days. $n = 4$ per group.

(J) qRT-PCR analysis of RSPO2 and *ID1* in THP-1 clones upon Dox treatment for 3 days. $n = 4$ per group.

(K) Western blot analysis of pSmad1 and tSmad1 in THP-1 clones upon Dox treatment for 3 days.

Results are presented as the mean \pm SD. ** $p < 0.01$, *** $p < 0.001$, and **** $p < 0.0001$ from unpaired *t* test for experiments with two groups or one-way ANOVA for experiments with more than two groups. See also Figure S1.



(legend on next page)

expression, while RSPO2 recombinant protein and/or conditioned medium (CM) treatment reverted these effects (Figures 1H and 1I).

To corroborate these observations, we established two THP-1 clones expressing Doxycycline (Dox)-inducible shRSPO2 RNA (TetOn-shRSPO2). Consistently, Dox administration reduced cytosolic β -catenin levels and induced BMP signaling (Figures S1L, 1J, and 1K). Additional treatment of the two THP-1 clones with RSPO2 inhibited BMP signaling, attesting to the specificity of the shRSPO2 RNA (Figures S1M–S1P). We extended these results in MOLM14 monocytic leukemia (M5; MLL-AF9 fusion) cells, which also showed increased *ID1* expression and Smad1-phosphorylation upon knockdown of *RSPO2* (Figures S1Q and S1R). Collectively, these results indicate that AML cells possess active RSPO2 and thereby inhibit endogenous BMP signaling.

Autocrine RSPO2 blocks AML cell differentiation by inhibiting BMP signaling

AML arises from uncontrolled proliferation and impaired differentiation of myeloid precursors (Nowak et al., 2009), raising the possibility that *RSPO2*, via reducing BMP signaling and thereby inhibiting myeloid differentiation, could act as an endogenous oncogene in AML cells. Since BMP signaling inhibits self-renewal and induces differentiation of THP-1 cells into macrophages (Pardali et al., 2018; Rocher et al., 2012), we asked whether *RSPO2* knockdown in THP-1 cells could do the same (Figure 2A). Strikingly, siRSPO2 RNA treatment increased RNA as well as protein levels of the macrophage markers *CD14* and *CD11B* (Figures 2B–2D), as did BMP4 treatment (Figures 2E and 2F). Likewise, not only transient siRNA, but also Dox treatment, in TetOn-shRSPO2 clones induced expression of *CD14* and *CD11B* (Figure S2A). An alternative loss-of-function approach using neutralizing Abs targeting endogenous RSPO2 showed similar effects (Figures S2B and S2C). Morphologically, sustained shRSPO2 expression reduced the nuclear-cyto-

plasmic ratio of THP-1 cells, indicative of cell differentiation (Figure S2D), supporting that RSPO2 maintains THP-1 cells undifferentiated. Conversely, recombinant RSPO2 reverted the effect of siRSPO2 on *CD14* and *CD11B* expression (Figures S2E and S2F). Moreover, we stimulated cells with ATRA, which induces macrophage differentiation in a number of monocytic cell lines, including THP-1 cells (Chen and Ross, 2004). ATRA treatment enhanced *CD11B* expression, while co-treatment with RSPO2 recombinant protein or CM reverted this effect (Figures 2G and S2G).

We used the ATRA treatment to corroborate that RSPO2 functions as a BMP antagonist rather than a WNT agonist in this signaling context. We produced recombinant RSPO2 proteins lacking either the FU1 or the FU2 domains, which mediate binding to ZNRF3/RNF43 and LGRs, respectively (Lee et al., 2020; Szenker-Ravi et al., 2018). We previously showed that RSPO2^{ΔFU2}, but not RSPO2^{ΔFU1}, antagonizes BMP signaling in a BMP reporter assay, while WNT stimulation requires both FU1 and FU2 domains (Lee et al., 2020). Here, we treated THP-1 cells with ATRA, which induced *ID1* and *CD11B* expression (Figure 2G). While wild-type (WT) RSPO2 reduced *ID1* and *CD11B* expression, the FU1 deletion expectedly failed to revert these effects, as it cannot engage ZNRF3. By contrast, the FU2 deletion reduced *ID1* and *CD11B* expression similar to WT. This experiment provides compelling evidence for LGR4/5/6—and, hence, WNT signaling—interdependence.

While RSPO2 treatment impaired ATRA-mediated differentiation, knockdown of *RSPO2* cooperated with ATRA in inducing differentiation (Figure S2H). In not only THP-1 cells, but also MOLM14 cells, *RSPO2* knockdown increased *CD14* and *CD11B* mRNA expression as well as *CD11B* protein levels, affirming the inhibitory role of RSPO2 in AML cell differentiation (Figures 2H–2J). Differentiated MOLM14 cells displayed vacuolar structures and increased cell size (from $37.3 \pm 1.9 \mu\text{M}^2$ to $44.1 \pm 2.9 \mu\text{M}^2$) (Figure S2I). In contrast, *RSPO2* knockdown in U937 cells (M4/M5-AML; CALM/AF10 fusion) showed no to

Figure 2. RSPO2 prevents differentiation of AML cells

(A) Experimental scheme of AML cell differentiation.

(B) qRT-PCR analysis of macrophage markers *CD14* and *CD11B* in siRNA-treated THP-1 cells. $n = 4$ per group.

(C) FACS plots for *CD14*⁺ or *CD11B*⁺ cells upon siRNA transfection of THP-1 cells.

(D) Quantification of FACS analysis for *CD14*⁺ or *CD11B*⁺ cells upon siRNA transfection of THP-1 cells. Positive cells were defined based on the signals of isotypic control staining. $n = 3$ per group.

(E) FACS plots for *CD14*⁺ cells in THP-1 cells following overnight stimulation by 5 and 25 ng/ml BMP4.

(F) Quantification of FACS analysis for *CD14*⁺ cells in THP-1 cells following BMP4 stimulation. $n = 3$ per group.

(G) qRT-PCR analysis of *ID1* and *CD11B* in THP-1 cells upon treatment with 10 nM ATRA and CM of RSPO2 FU1 and FU2 deletion variants for 3 days. $n = 4$ per group. R2, RSPO2.

(H) qRT-PCR analysis of *CD14* and *CD11B* in MOLM14 clones upon Dox treatment for 3 days. $n = 3$ per group.

(I) FACS plots for *CD11B*⁺ cells in MOLM14 clones upon Dox treatment for 7 days.

(J) Quantification of FACS analysis for *CD11B*⁺ cells in MOLM14 clones upon Dox treatment. $n = 3$ per group.

(K) Quantification of FACS analysis for *CD14*⁺ cells in siRNA-transfected THP-1 cells treated with BMP receptor inhibitor LDN. Cells were stimulated by 100, 300, and 1,000 nM LDN for 2 days before analysis. $n = 3$ per group. LDN, LDN-193189.

(L and M) Quantification of FACS analysis for *CD14*⁺ and *CD11B*⁺ cells in siRNA-transfected THP-1 cells treated with BMP receptor inhibitor DMH2. Cells were stimulated by 100, 300, and 1,000 nM DMH2 for 2 days before *CD14* analysis (L). Cells were stimulated by 100 and 300 nM DMH2 for 2 days before *CD11B* analysis (M). $n = 3$ per group.

(N) qRT-PCR analysis of the indicated genes in THP-1 cells treated as indicated. Cells were stimulated overnight by the same relative high amount of WNT3A and DKK1 shown in Figure S2Q or 1 μM XAV. XAV, XAV 939. $n = 4$ per group.

(O) qRT-PCR analysis of the indicated genes in THP-1 cells. Cells were stimulated by 1 and 10 μM IWP-2 or 10 nM ATRA. $n = 4$ per group.

Results are presented as the mean \pm SD. ns, not significant; * $p < 0.05$, ** $p < 0.01$, *** $p < 0.001$, and **** $p < 0.0001$ from unpaired t test for experiments with two groups or one-way ANOVA for experiments with more than two groups. See also Figure S2.

mild increase of *ID1*, *CD14*, and *CD11B* expression upon Dox treatment, and no substantial differentiation was observed in fluorescence-activated cell sorting (FACS) analysis (Figures S2J and S2K). We conclude that RSPO2 blocks differentiation in a subset of AML cell lines.

To address if THP-1 differentiation induced by RSPO2 deficiency resulted from upregulated BMP signaling, we utilized the BMP receptor inhibitors LDN 193189 (Cuny et al., 2008) and DMH2 (Hao et al., 2010), whose administration decreased BMP signaling (Figures 1C and S2L). Attenuating BMP receptor signaling impaired differentiation into macrophages induced by siRSPO2 (Figures 2K–2M). In contrast, treatment with WNT3A, DKK1 (Glinka et al., 1998), the Axin-stabilizer XAV939 (Huang et al., 2009), or the porcupine inhibitor IWP-2 (Chen et al., 2009) did not significantly alter BMP signaling as well as *CD14* and *CD11B* RNA or protein levels (Figures 2N, 2O, and S2M–S2P), despite all treatments affecting WNT signaling in THP-1 cells (Figures S2Q–S2S). In addition, RSPO2 treatment reverted ATRA-induced *ID1* and *CD11B* in the presence of IWP-2 (Figure S2T). These results corroborate that RSPO2 prevents AML cell differentiation by inhibiting BMP signaling instead of activating WNT signaling.

Autocrine RSPO2 maintains AML cell proliferation and contributes to AraC resistance

Previous studies showed that BMP signaling activation induces growth inhibition and differentiation in certain leukemia cells (Imai et al., 2001; Jiang et al., 2000; Wang et al., 2006). Given that RSPO2 inhibits BMP signaling and blocks differentiation, we postulated that RSPO2 might regulate growth of AML cells. To test this possibility, we analyzed the proliferation of TetOn-shRSPO2 THP-1 cells and found that Dox administration reduced cell growth (Figure 3A). Cell-cycle analysis using bromodeoxyuridine/propidium iodide (BrdU/PI) staining revealed a G0/G1 arrest in TetOn-shRSPO2 cells after Dox treatment, while the percentage of cells in S and G2/M phases was decreased (Figure 3B). Additionally, knockdown of RSPO2 decreased colony formation of THP-1 and MOLM14 cells (Figures 3C–3G), without inducing apoptosis (Figure 3H). The growth-inhibitory effect of shRSPO2 RNA was partially reverted by treatment with RSPO2 as well as the BMP receptor inhibitor LDN 193189 (Figure S3A), while IWP-2 had little effect (Figure S3B). We conclude that autocrine RSPO2 is required to maintain THP-1 proliferation.

Cytarabine (AraC) treatment remains a major line of chemotherapy in AML but suffers from resistant disease during relapse (Döhner et al., 2015). To test whether RSPO2 expression is related to drug resistance, we measured the half-inhibitory concentration (IC₅₀) of AraC in multiple AML cell lines expressing RSPO2 (Figure S1A). Interestingly, mRNA levels of RSPO2, but not RSPO1, were positively correlated with the AraC-IC₅₀ (Figures S3C and S3D). To test directly whether RSPO2 promotes AraC resistance, we determined the IC₅₀ of AraC in a TetOn shRSPO2 THP-1 clone and found that Dox administration in shRSPO2 cells reduced IC₅₀ of AraC by half (Figure 3I). Moreover, co-treatment of Dox and AraC significantly reduced cell growth compared to single treatment (Figure S3E). Taken together, we conclude that autocrine RSPO2 maintains proliferation of THP-1 cells and modulates their AraC sensitivity.

RSPO2 is required for primary HSPC and AML-LSC maintenance

HSPCs and primary cells from patients with AML require growth factors and cytokines from the bone marrow niche for survival and growth (Konopleva and Jordan, 2011), leading to their spontaneous differentiation *in vitro*. To explore the role of RSPO2 in self-renewal of HSPC as well as primary cells from a PDX model *in vitro*, we analyzed CD34⁺ cells from cord blood and PDX-AML-661 cells (Ebinger et al., 2020) upon RSPO2 RNA knockdown (Figure 4A). Lentiviral shRSPO2 expression slightly reduced the fraction of less-differentiated HSPCs (CD34⁺, CD45RA[−]) and increased the number of differentiated progenitors (CD34⁺, CD45RA⁺) (Figure 4B). In AML-661 cells, RSPO2 knockdown led to a more pronounced reduction of the LSC pool (CD34⁺), notably upon prolonged (20-day) cultivation (Figure 4C). Consistently, RSPO2 knockdown slightly decreased cell proliferation of cord blood cells (CD34⁺) and more so in AML-661 cells (Figure 4D). Conversely, RSPO2 knockdown increased the percentage of differentiated (CD14⁺, CD11B⁺) cells, slightly in cord blood, and more pronounced in AML-661 cells (Figure 4E). In colony formation assays, knockdown of RSPO2 in normal HSPCs reduced total colony number, including BFU-E (burst-forming erythroid), CFU-G (granulocyte), and the most immature CFU-GEMM (granulocyte, erythroid, macrophage, megakaryocyte) forming precursors, while it increased the number of CFU-M (macrophage), but had no effect on CFU-GM (granulocyte-macrophage) (Figure 4F). Further flow cytometry analysis on cells collected from colony formation assays showed a significant increase of CD14⁺ CD11B⁺ cells in the shRSPO2 group (Figure S4A).

We analyzed the involvement of RSPO2 during myeloid differentiation and induced mouse bone marrow cells with macrophage colony-stimulating factor (M-CSF) (Figure 4G). *Rspo2* knockdown upregulated BMP signaling (*ID1* expression and pSmad1) (Figures 4H and S4B) and enhanced differentiation into macrophages, increasing the number of CD11B⁺ F4/80⁺ cells (Figure 4I). Morphologic analysis revealed an increase in the number of macrophages after si*Rspo2* treatment (Figure S4C). Importantly, BMPR inhibitor LDN 193189 treatment reverted macrophage differentiation induced by si*Rspo2* (Figure 4J). In contrast, RSPO2 knockdown did not impair differentiation of peripheral blood human monocytes into macrophages (Figures 4K, S4D, and S4E), despite increased *ID1* expression (Figure S4F). Collectively, these data support that RSPO2 deficiency has no effect on normal monocyte-to-macrophage differentiation, a modest effect on HSPCs' self-renewal, and a more pronounced effect on maintenance of AML cell self-renewal. Hence, the results support a role for autocrine RSPO2 signaling in normal HSPCs and primary AML cell renewal.

Elevated RSPO2 expression predicts poor prognosis in AML

The role of RSPO2/BMP signaling in promoting AML self-renewal and AraC resistance *in vitro* raised the possibility that RSPO2 expression levels correlate with, and may be predictive for, patient prognosis. Hence, we carried out datamining utilizing multiple AML cohorts. We first compared the expression of

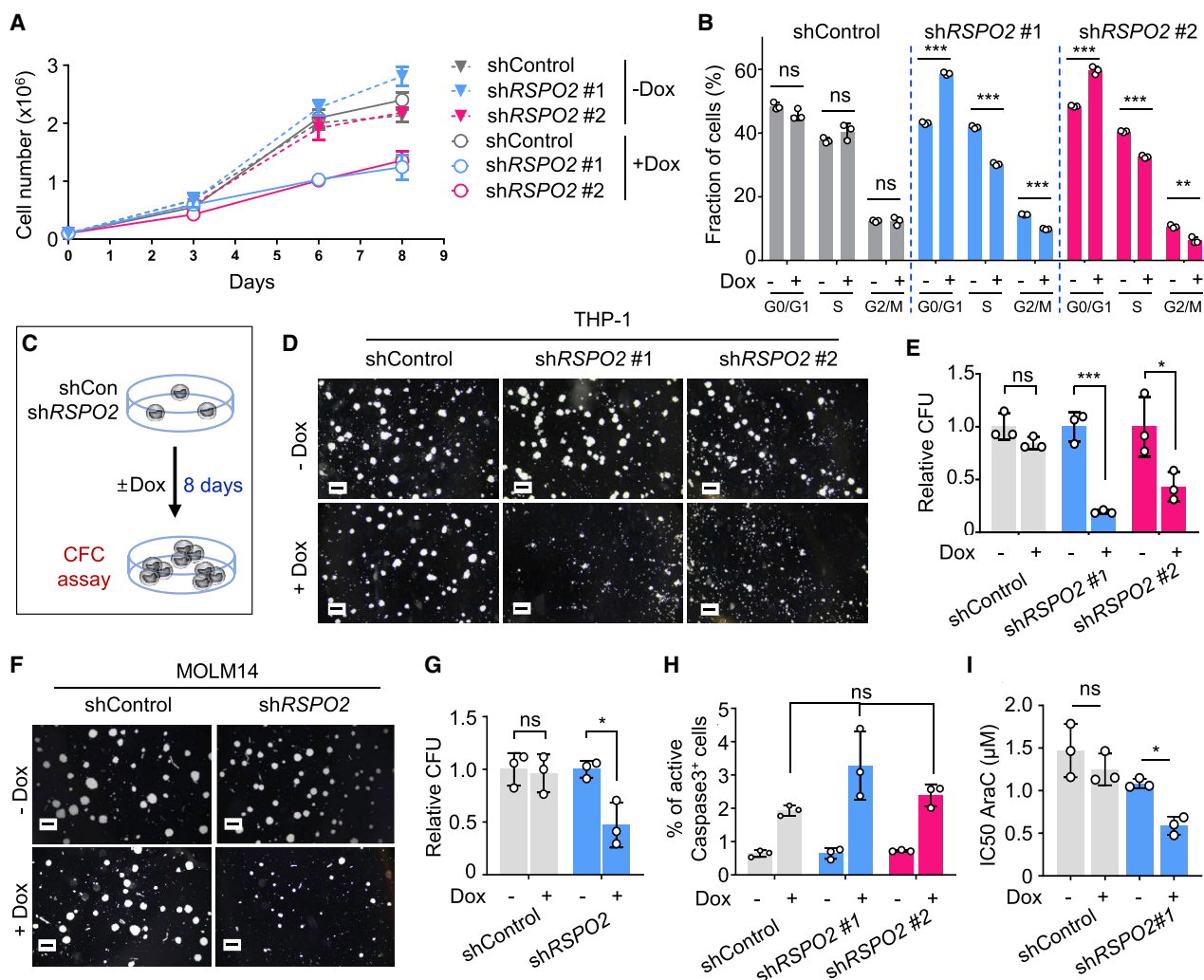


Figure 3. RSP02 is required for proliferation of AML cells

(A) Cumulative cell growth curve depicted as the total cell count of THP-1 shRNA cell lines with Dox treatment. Cell number was counted at the indicated time points with automated cell counter and normalized to the initial value. $n = 3$ per group.

(B) Cell-cycle FACS analysis using BrdU/PI double staining of THP-1 shRNA cell lines. Cells were treated with Dox for 4 days and incubated with 10 μM BrdU for 1 h before FACS analysis. $n = 3$ per group. PI, propidium iodide.

(C) Experimental scheme of colony formation cell (CFC) assay with Dox-inducible shRNA THP-1 cell lines.

(D) Representative images of CFC assay of THP-1 colonies. Scale bar, 200 μM.

(E) Quantification of THP-1 CFC assay. $n = 3$ per group.

(F) Representative images of CFC assay of MOLM14 colonies. Scale bar, 200 μM.

(G) Quantification of MOLM14 CFC assay. $n = 3$ per group.

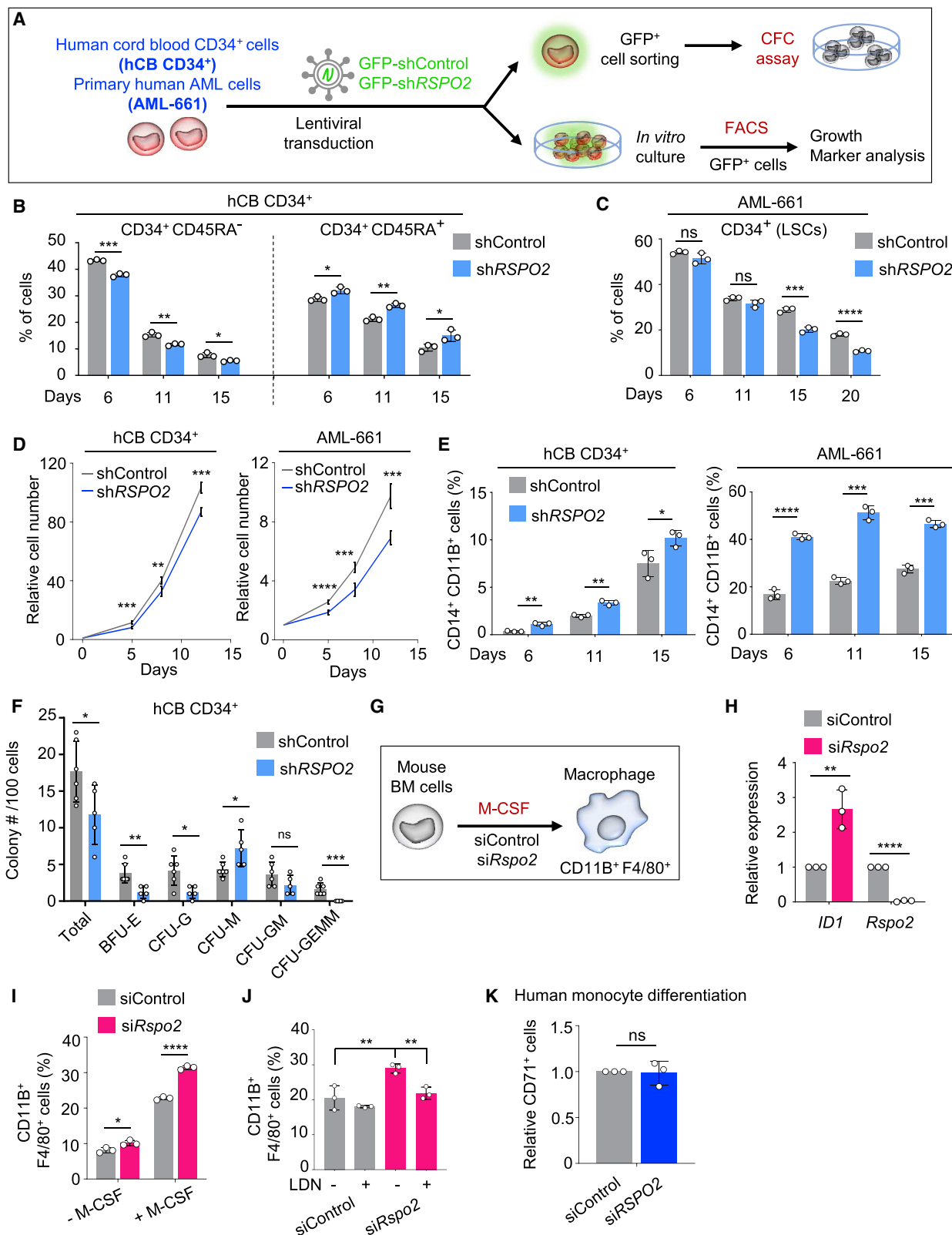
(H) Quantification of FACS analysis for active caspase-3⁺ cells in THP-1 clones with Dox treatment for 3 days. Cells were fixed by paraformaldehyde (PFA) and permeabilized with MeOH before Ab staining. $n = 3$ per group.

(I) AraC IC₅₀ of THP-1 clones upon Dox treatment. TetOn shRSP02 cells were pretreated with Dox for 2 days. IC₅₀ was determined after 3 days incubation with increasing amount of AraC in the presence of Dox as indicated. $n = 3$ per group.

Results are presented as the mean ± SD. ns, not significant; * $p < 0.05$, ** $p < 0.01$, *** $p < 0.001$ from unpaired t test for experiments with two groups or one-way ANOVA for experiments with more than two groups. See also Figure S3.

RSP0s between healthy and AML samples (Corces et al., 2016; Tyner et al., 2018). RSP02 mRNA levels were systematically elevated in AML samples compared to normal HSPCs (Figure 5A). Moreover, RNA sequencing with sorted primary AML cells revealed that higher RSP02 mRNA levels reside in LSCs, but not in preleukemic hematopoietic stem cells (pHSC) or

leukemic blast cells (Blast) (Figure 5B). We then stratified the expression of RSP0s in different patient risk groups. Using GDC-TCGA data, we found that expression of RSP02 and RSP04, but not of RSP01 and RSP03, was higher in intermediate and poor risk groups compared to the favorable risk group (Figure 5C). Elevated RSP02 expression in intermediate or



(legend on next page)

adverse groups was also observed in the BEAT and TARGET AML cohorts (Bolouri et al., 2018; Tyner et al., 2018; Figures 5D and 5E). These data indicate that elevated *RSPO2* expression generally correlates with poor disease status.

Analysis of overall survival in the GDC-TCGA AML cohort revealed that high *RSPO2* expression was a superior predictor for poor prognosis (hazard ratio [HR] 2.018; $p = 0.0014$) compared to commonly used markers (*HOXA9*, HR 1.899; $p = 0.0034$; *PBX3*, HR 2.011; $p = 0.0014$; *MEIS1*, HR 1.460; $p = 0.0304$; *MECOM*, HR 0.6913; $p = 0.0948$) (Goldman et al., 2019; Lugthart et al., 2008; Zhu et al., 2017; Figures S5A–S5H). Conversely, low-level expression of *BMP4/5* was associated with decreased survival (Figures S5I and S5J). In contrast, high expression of *RSPO1* and *RSPO3*, as well as the WNT target genes *MYC* and *AXIN2*, was not correlated with poor survival (Figures S5A, S5C, S5K, and S5L). *RSPO2* as a marker for poor prognosis was further validated with three other cohorts of patients with AML, BEAT, TARGET, and leucegene. Higher *RSPO2* expression positively correlated with poor survival of patients with AML in all cases, while expression of *RSPO1*, *RSPO3*, and *RSPO4* showed no systematic correlation with patient survival (Figures 5F–5H). Finally, *RSPO2* expression did not correlate with patient age-at-diagnosis (Figures 5I and 5J). Altogether, the results indicate that elevated *RSPO2* expression is generally associated with adverse risk and poor prognosis in AML.

Loss of autocrine *RSPO2* signaling prolongs survival of AML xenograft mice

We finally investigated the putative therapeutic effect of inhibiting *RSPO2* to restrict disease progression in AML xenograft models. We first injected TetOn-sh*RSPO2* or TetOn-shControl THP-1 cells into immunodeficient NOD scid gamma (NSG) mice (Figure 6A). Mice harboring TetOn-shControl THP-1 cells rapidly developed leukemia and reached humane endpoint within 50 days post-injection, with or without Dox treatment (Fig-

ure 6B). Mice injected with the two TetOn-sh*RSPO2* THP-1 cell lines (#1, #2) also reached the humane endpoint between 42 and 62 days without Dox treatment. In contrast, upon Dox treatment, mice injected with cell line #2 survived almost twice as long, and the majority of mice injected with line #1 appeared normal before day 160, corresponding to a 3-fold prolongation of disease-free survival (Figures 6B and 6C). Extended survival was accompanied by reduced tumor burden (Figures 6D, 6E, and S6A–S6E) and enhanced differentiation of tumor cells (Figure 6F).

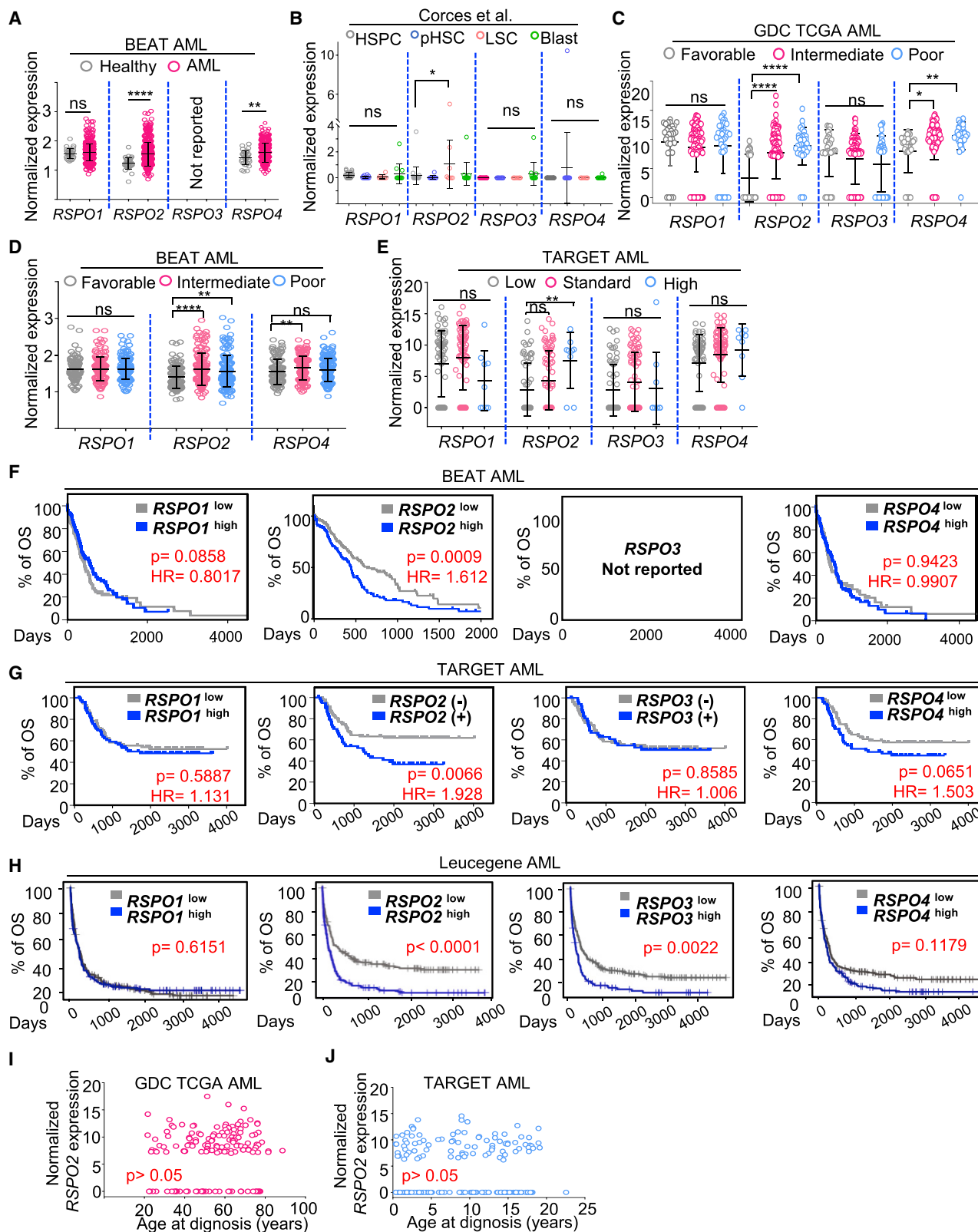
We next injected primary AML-661 cells lentivirally transduced with GFP and sh*RSPO2* into NSG mice (Figure 6G). After 63 days, we sacrificed the mice and performed a bone marrow analysis. Consistent with our liquid culture data, *RSPO2* deficiency reduced the engraftment efficiency, as shown by decreased percentage of GFP⁺ cells in the sh*RSPO2* group (Figure 6H). Marker analysis revealed that LSCs (CD34⁺ cells) were markedly reduced upon sh*RSPO2* expression (Figure 6I), while differentiated cells (CD14⁺ CD11b⁺ cells) were increased (Figure 6J). Together, these results corroborate the importance of *RSPO2* in maintaining aggressive AML *in vivo*.

DISCUSSION

Understanding extracellular signals regulating self-renewal in AML cells is essential for designing effective cancer therapies, yet they remain incompletely understood. The main finding of this study is that *RSPO2* promotes cancer cell self-renewal in AML by inhibiting BMP signaling. The data emphasize the role of the BMP pathway in promoting AML differentiation and provide a preclinical example for the function of *RSPO2* as a BMP antagonist rather than a WNT agonist. We also demonstrate that *RSPO2* expression is a powerful predictor for AML disease progression. Altogether, the results recommend *RSPO2* as a prognostic marker as well as a target for differentiation therapy in AML.

Figure 4. *RSPO2* maintains HSPC and AML-LSC self-renewal and prevents their differentiation via BMP inhibition

- (A) Scheme of experimental setup for human primary cord blood CD34⁺ cells and PDX AML-661 cell analysis.
- (B) Quantification of FACS analysis for indicated markers of cord blood CD34⁺ cells cultivated *in vitro* for different days after lentiviral infection. Only GFP-expressing cells were analyzed. $n = 3$ per group.
- (C) Quantification of FACS analysis of AML-661 cells cultivated *in vitro* for different days after lentiviral infection. Only GFP-expressing cells were analyzed. $n = 3$ per group.
- (D) Cumulative cell growth curve depicted as total cell count of cord blood CD34⁺ cells and AML-661 cells after lentiviral infection. Cell number in equal amount of medium volume was counted at the indicated time points with a flow cytometer equipped with a high-throughput sampler (HTS) device. Only GFP-expressing cells were analyzed. $n = 5$ per group.
- (E) Quantification of FACS analysis for indicated markers of cord blood CD34⁺ cells and AML-661 cells at different days as indicated after lentiviral infection. Only GFP-expressing cells were analyzed. $n = 3$ per group.
- (F) CFC assay with sorted GFP-positive cord blood CD34⁺ cells after lentiviral infection. BFU-E (burst-forming erythroid), CFU-G/M/GM (granulocyte/macrophage, granulocyte-macrophage), and CFU-GEMM (granulocyte, erythroid, macrophage, megakaryocyte) colony forming units scored by morphology. $n = 5/6$ per group.
- (G) Scheme of experimental setup for macrophage differentiation of mouse bone marrow.
- (H) qRT-PCR expression analysis of mouse bone marrow cells for indicated genes after siRNA transfection. $n = 3$ per group.
- (I) Quantification of FACS analysis for indicated markers of mouse bone marrow cells after siRNA transfection. Bone marrow cells were stimulated by 20 ng/ml murine M-CSF for 3 days before analysis. $n = 3$ per group.
- (J) Quantification of FACS analysis for indicated markers of mouse bone marrow cells treated with siRNA and LDN 193189 as indicated. Bone marrow cells were stimulated by 20 ng/ml murine M-CSF with or without 100 nM LDN 193189 for 3 days before analysis. $n = 3$ per group.
- (K) Human monocyte-to-macrophage differentiation assay. Quantification of FACS analysis for CD71⁺ in purified primary human monocytes treated with siRNA as indicated. Monocytes were stimulated by 100 ng/ml human M-CSF for 2 days before analysis. Data were pooled from three different blood donors. Results are presented as the mean \pm SD. ns, not significant; * $p < 0.05$, ** $p < 0.01$, *** $p < 0.001$, **** $p < 0.0001$, from unpaired t test. See also Figure S4.



(legend on next page)

Autocrine RSPO2 inhibits BMP signaling to promote AML self-renewal

BMP signaling is a regulator in normal hematopoiesis and AML progression. BMP/SMAD5 signaling inhibits proliferation and induces differentiation of HSPCs and AML cells (Bhatia et al., 1999; Detmer and Walker, 2002; Fuchs et al., 2002; Jiang et al., 2000; Liu et al., 2003; Wang et al., 2006). In addition, loss-of-function mutations in *SMAD4* contribute to AML pathogenesis (Imai et al., 2001). We show that RSPO2 deficiency induces BMP signaling, which impairs the self-renewal of AML cells, promotes their macrophage differentiation, and abates AML progression in xenograft models. However, while we found that RSPO2 deficiency moderately enhanced myeloid differentiation of HSPCs, it did not promote normal monocyte-to-macrophage differentiation, suggesting instead a role of RSPO2 specifically in monocyte precursors, consistent with elevated *RSPO2* expression in LSCs.

While there is evidence that BMP signaling can also have the opposite function in AML—maintaining the stem cell pool and promoting cell proliferation—closer inspection indicates that this oncogenic role may be restricted to specific AML subtypes. For example, BMP signaling is required for the AML subtype AMKL (pediatric acute megakaryoblastic leukemia), where a rare *CBFA2T3-GLIS2* gene fusion not found in adults induces proliferation via BMP signaling (Gruber et al., 2012). Moreover, BMP signaling inhibits differentiation in acute promyelocytic leukemia (APL), which accounts for 5% to 8% of cases of AML (Topić et al., 2013). Similarly, BMP inhibitor treatment of a variety of AML lines is detrimental only to those expressing the *MIXL1* oncogene (Raymond et al., 2014). Hence, whether BMP signaling promotes self-renewal or differentiation may vary with AML subtype. Assuming that the widespread elevation of *RSPO2* expression and correlation with poor prognosis observed in patients with AML reflects its role in suppressing BMP signaling, our results support the view that in the majority of AML cases, the BMP pathway is tumor suppressive.

Recently, the RSPO receptor LGR4 was shown to promote self-renewal in a subset of AML, and RSPO3 acts as a stem cell growth factor to sustain proliferation of AML LSCs dependent on LGR4 (Salik et al., 2020). The study reported that blocking the RSPO3-LGR4 signaling axis by RSPO3-neutralizing Abs retards leukemia disease progression. It was proposed that RSPO-LGR4 acts via WNT signaling, consistent with a role of the pathway in AML (Gruber et al., 2012; Majeti et al., 2009; Wang et al., 2010; Yeung et al., 2010). Hence, collectively, these results suggest that multiple RSPOs may promote AML self-renewal in autocrine fashion and by more than one signaling

mechanism, supporting that these secreted effectors represent attractive drug targets in AML.

The role of RSPO2 in normal hematopoiesis is unknown. We found a modest requirement of RSPO2 for maintenance of undifferentiated HSPCs *in vitro*, which became more manifest in colony formation assays. Consistently, in human embryonic stem cells, the addition of RSPO2 enhances hematopoietic specification from pluripotent stem cells (Wang et al., 2019) and promotes proliferation of hematopoietic precursors (Desterke et al., 2020). However, these data are based on *in vitro* studies, which monitor predominantly autocrine signaling and may not faithfully recapitulate HSC self-renewal *in vivo*. Notably, RSPO2 is a top candidate for a mesenchymal-stromal-secreted cytokine (Desterke et al., 2020), raising the possibility that in addition to autocrine RSPO2 signaling in HSPC and AML cells as analyzed here, there may be a paracrine contribution from the bone marrow niche. Clearly, the requirement of RSPO2 in normal hematopoiesis and in AML needs to be further characterized in *in vivo* settings in the future.

RSPO2 as a prognostic marker and therapeutic target in AML

Another main conclusion of this study is that high *RSPO2* is predictive of poor outcome of patients with AML, supporting that our experimental findings may be of clinical relevance. The association of high *RSPO2* expression with poor outcome was robustly observed in all cohorts analyzed. We note that high *RSPO2* expression features a higher HR for adverse prognosis (overall survival) than the other commonly employed markers *HOXA9*, *MEIS1*, *PBX3*, and *MECOM* (Andreeff et al., 2008; De Kouchkovsky and Abdul-Hay, 2016; Dickson et al., 2013; Döhner et al., 2015; Golub et al., 1999; Lugthart et al., 2008; Zangenberg et al., 2009). Hence, monitoring *RSPO2* expression may aid in risk stratification and provide guidance to select patients (e.g., for cell transplant therapy).

RSPO2 is required for self-renewal of AML cells, both in cell lines and in PDX cells, and RSPO2 deficiency promotes their differentiation. Hence, as secreted effector, RSPO2 may be a candidate target for Ab-based therapy in AML. We found a greater susceptibility of AML cells compared to normal HSPCs to RSPO2 reduction, at least *in vitro*, raising the possibility that there may be a therapeutic window for such a therapy. Since RSPO2 signaling contributes to AraC resistance in THP-1 cells, RSPO2 reduction may be useful as adjuvant in combination with chemotherapeutics.

Further specificity for an anti-RSPO2 therapeutic reagent may be achieved by exploiting the fact that BMP inhibition and WNT activation reside on different domains of the RSPO2 protein.

Figure 5. High *RSPO2* expression is a predictor for adverse risk in AML

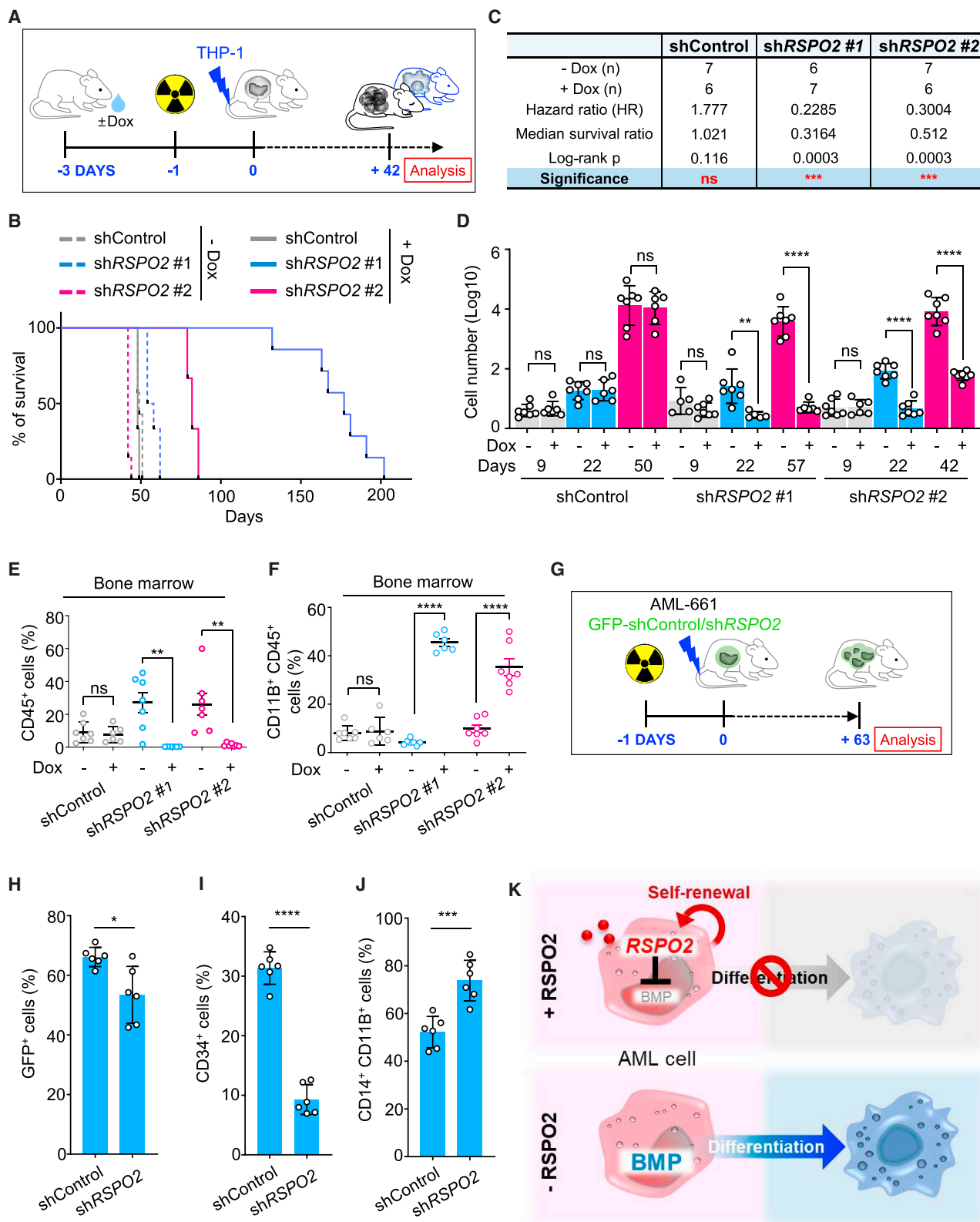
(A and B) Normalized *RSPO1-4* expression in healthy individuals and patients with AML from (A) BEAT AML (Tyner et al., 2018) and (B) Corces et al. (2016). Note, *RSPO3* expression was not reported in the BEAT AML database.

(C–E) Normalized *RSPO1-4* expression in different AML risk groups (low, standard, high) from GDC-TCGA AML (C), BEAT AML (D), and TARGET AML (E).

(F–H) Kaplan-Meier plot of patients with AML stratified by different gene expression levels in different databases: (F) BEAT, (G) TARGET, and (H) leucegene. OS, overall survival.

(I and J) Correlation between normalized *RSPO2* expression with patient age-at-diagnosis in years in (I) GDC-TCGA and (J) TARGET AML databases.

Results are presented as the mean \pm SD. ns, not significant; * $p < 0.05$, ** $p < 0.01$, **** $p < 0.0001$ from unpaired t test or one-way ANOVA. Log-rank test was used for survival analysis. See also Figure S5.



(legend on next page)

While WNT signaling requires the Furin domains, BMP inhibition resides in the TSP1 domain, which binds the BMP receptor ALK3. Indeed, the WNT-agonistic and BMP-antagonistic roles of RSPO2 can be uncoupled *in vivo* by deleting the TSP1 domain without affecting WNT signaling (Lee et al., 2020). Thus, by targeting the TSP1 domain selectively, the WNT agonist role of RSPO2 may be spared and side effects limited.

Looking beyond AML, RSPO2 is implicated in breast, pancreatic, gastric, and colorectal cancer (CRC), and its function is commonly thought to reside exclusively in its ability to activate WNT signaling (Ilmer et al., 2015; Klauzinska et al., 2012; Wu et al., 2014; Zhang et al., 2019). Given that RSPO2 antagonizes BMP signaling in AML, it is noteworthy that not only WNT activation, but also suppression of BMP signaling, are hallmarks of CRC (Wang and Chen, 2018). Hence, in light of the dual function as WNT activator and BMP suppressor, the mode of RSPO2 action in these cancer entities should be revisited.

STAR★METHODS

Detailed methods are provided in the online version of this paper and include the following:

- KEY RESOURCES TABLE
- RESOURCE AVAILABILITY
 - Lead contact
 - Materials availability
 - Data and code availability
- EXPERIMENTAL MODEL AND SUBJECT DETAILS
 - Cell lines and growth conditions
 - Primary cell culture
 - Animal experiments
- METHOD DETAILS
 - siRNA transfection
 - Generation of conditioned medium
 - TOPflash luciferase reporter assays
 - Western blot analysis
 - Quantitative real-time PCR
 - FACS analysis
 - RSPO2 antibody neutralization assay
 - Generation of inducible shRNA expressing cell lines

- Cell cycle analysis with BrdU/PI double staining
- Cytarabine/AraC IC₅₀ measurement and proliferation assay
- Colony formation assay with THP-1 and MOLM14 cells
- Lentivirus transduction of primary human cells and analysis
- Colony formation assay with primary cord blood CD34⁺ cells
- Mouse bone marrow cell analysis
- Primary monocyte analysis
- Cytospin and Wright-Giemsa staining
- *In vivo* THP-1 xenotransplantation into NSG mice and AML PDX experiments
- qPCR analysis for THP-1 burden in NSG mouse
- Expression analysis and Kaplan-Meier plot of patients with AML

● QUANTIFICATION AND STATISTICAL ANALYSIS

SUPPLEMENTAL INFORMATION

Supplemental information can be found online at <https://doi.org/10.1016/j.celrep.2021.109559>.

ACKNOWLEDGMENTS

We thank S. Wiemann for THP-1 cells; A. Trumpp for HL60, MV4-11, MOLM13, MOLM14, NB4, and U937 cells and for advice; and S. Fröhling for NOMO-1 cells. Model PDX AML-661 was established by B. Vick. We acknowledge F. da Silva for critical reading of the manuscript. Expert technical support by the DKFZ core facility for flow cytometry, light microscopy, and the central animal laboratory of DKFZ is gratefully acknowledged. This work was supported by the Deutsche Forschungsgemeinschaft (CRC 1324). C.P. is supported by Deutsche Forschungsgemeinschaft (DFG PA2815/1-1) and by a Max-Eder-Grant of the German Cancer Aid (70111531).

AUTHOR CONTRIBUTIONS

R.S. designed and carried out cell line experiments, primary cell experiments with L.H., and mouse experiments with K.M.-D. H.L. helped in mouse experiments and generated illustrations. A.G. generated materials for the study. R.S., C.A., and D.H. performed datamining analysis. I.J. provided the established AML-661 PDX model. C.P. supervised primary cell experiments (cord blood cells and AML PDX cells) and provided reagents. C.N. conceived and coordinated the study and wrote the paper with contributions from R.S. and H.L.

Figure 6. Loss of RSPO2 prolongs survival in AML xenograft models

- (A) Scheme of THP-1 xenografts in mice.
- (B) Survival plot of mice xenografted with THP-1 cell lines expressing the indicated Dox-inducible short hairpin RNAs (shRNAs). Death event was recognized once reaching the humane endpoint.
- (C) Table showing the number of mice analyzed (n), hazard ratio (HR), median survival ratio, and significance of survival differences in mice xenografted with THP-1 cell lines expressing the indicated Dox-inducible shRNAs.
- (D) *Alu* element qPCR analysis of the THP-1 burden in peripheral blood. Genomic DNA was isolated from peripheral blood sampled at indicated time point through tail vein bleeding. For each qPCR reaction, an equal amount of genomic DNA was used.
- (E) Quantification of FACS analysis for THP-1 cell number in mouse bone marrow using human-specific CD45 Ab.
- (F) Quantification of FACS analysis for CD11B⁺ CD45⁺ cells in mouse bone marrow. Samples were analyzed on day 50 post-cell-injection for shControl, day 57 post-cell-injection for shRSPO2-1, and day 42 post-cell-injection for shRSPO2-2 separately. Samples from Dox-treated and untreated groups were analyzed at the same time.
- (G) Scheme of AML-661 PDX xenograft experiment.
- (H) Quantification of FACS analysis for GFP⁺ AML-661 cells in mouse bone marrow after gating on CD45⁺ cells using a human-specific CD45 Ab. n = 6 per group.
- (I) Quantification of FACS analysis for CD34⁺ AML-661 cells in mouse bone marrow after gating on CD45⁺ and GFP⁺ cells. n = 6 per group.
- (J) Quantification of FACS analysis for CD14⁺ CD11B⁺ AML-661 cells in mouse bone marrow after gating on CD45⁺ and GFP⁺ cells. n = 6 per group.
- (K) Model for autocrine RSPO2 function to maintain AML cells undifferentiated by antagonizing BMP/ALK signaling.
- Results are presented as the mean ± SD. **p < 0.01, ***p < 0.001, ****p < 0.0001 from unpaired t test or log-rank test for survival analysis. See also Figure S6.

DECLARATION OF INTERESTS

C.N., R.S., and H.L. are listed in a pending patent based on this study.

Received: March 9, 2021

Revised: June 18, 2021

Accepted: July 28, 2021

Published: August 17, 2021

REFERENCES

- Acebron, S.P., Karaulanov, E., Berger, B.S., Huang, Y.L., and Niehrs, C. (2014). Mitotic wnt signaling promotes protein stabilization and regulates cell size. *Mol. Cell* 54, 663–674.
- Andreiff, M., Ruvo, V., Gadgil, S., Zeng, C., Coombes, K., Chen, W., Kornblau, S., Barón, A.E., and Drabkin, H.A. (2008). HOX expression patterns identify a common signature for favorable AML. *Leukemia* 22, 2041–2047.
- Antebi, Y.E., Linton, J.M., Klumpe, H., Bintu, B., Gong, M., Su, C., McCardell, R., and Elowitz, M.B. (2017). Combinatorial signal perception in the BMP pathway. *Cell* 170, 1184–1196.e24.
- Auwerx, J. (1991). The human leukemia cell line, THP-1: a multifaceted model for the study of monocyte-macrophage differentiation. *Experientia* 47, 22–31.
- Balgobind, B.V., Zwaan, C.M., Pieters, R., and Van den Heuvel-Eibrink, M.M. (2011). The heterogeneity of pediatric MLL-rearranged acute myeloid leukemia. *Leukemia* 25, 1239–1248.
- Berger, B.S., Acebron, S.P., Herbst, J., Koch, S., and Niehrs, C. (2017). Parkinson's disease-associated receptor GPR37 is an ER chaperone for LRP6. *EMBO Rep.* 18, 712–725.
- Bhatia, M., Bonnet, D., Wu, D., Murdoch, B., Wrana, J., Gallacher, L., and Dick, J.E. (1999). Bone morphogenetic proteins regulate the developmental program of human hematopoietic stem cells. *J. Exp. Med.* 189, 1139–1148.
- Bolouri, H., Farrar, J.E., Triche, T., Jr., Ries, R.E., Lim, E.L., Alonzo, T.A., Ma, Y., Moore, R., Mungall, A.J., Marra, M.A., et al. (2018). The molecular landscape of pediatric acute myeloid leukemia reveals recurrent structural alterations and age-specific mutational interactions. *Nat. Med.* 24, 103–112.
- Carmon, K.S., Gong, X., Lin, Q., Thomas, A., and Liu, Q. (2011). R-spondins function as ligands of the orphan receptors LGR4 and LGR5 to regulate Wnt/beta-catenin signaling. *Proc. Natl. Acad. Sci. USA* 108, 11452–11457.
- Chang, C. (2016). Agonists and antagonists of TGF-beta family ligands. *Cold Spring Harb. Perspect. Biol.* 8, a021923.
- Chartier, C., Raval, J., Axelrod, F., Bond, C., Cain, J., Dee-Hoskins, C., Ma, S., Fischer, M.M., Shah, J., Wei, J., et al. (2016). Therapeutic targeting of tumor-derived R-Spondin attenuates beta-catenin signaling and tumorigenesis in multiple cancer types. *Cancer Res.* 76, 713–723.
- Chen, Q., and Ross, A.C. (2004). Retinoic acid regulates cell cycle progression and cell differentiation in human monocytic THP-1 cells. *Exp. Cell Res.* 297, 68–81.
- Chen, B., Dodge, M.E., Tang, W., Lu, J., Ma, Z., Fan, C.W., Wei, S., Hao, W., Kilgore, J., Williams, N.S., et al. (2009). Small molecule-mediated disruption of Wnt-dependent signaling in tissue regeneration and cancer. *Nat. Chem. Biol.* 5, 100–107.
- Corces, M.R., Buenrostro, J.D., Wu, B., Greenside, P.G., Chan, S.M., Koenig, J.L., Snyder, M.P., Pritchard, J.K., Kundaje, A., Greenleaf, W.J., et al. (2016). Lineage-specific and single-cell chromatin accessibility charts human hematopoiesis and leukemia evolution. *Nat. Genet.* 48, 1193–1203.
- Cruz, A.C.C., Cardozo, F.T.G.S., Magini, R.S., and Simões, C.M.O. (2019). Retinoic acid increases the effect of bone morphogenetic protein type 2 on osteogenic differentiation of human adipose-derived stem cells. *J. Appl. Oral Sci.* 27, e20180317.
- Cuny, G.D., Yu, P.B., Laha, J.K., Xing, X., Liu, J.F., Lai, C.S., Deng, D.Y., Sachidanandan, C., Bloch, K.D., and Peterson, R.T. (2008). Structure-activity relationship study of bone morphogenetic protein (BMP) signaling inhibitors. *Bioorg. Med. Chem. Lett.* 18, 4388–4392.
- De Kouchkovsky, I., and Abdul-Hay, M. (2016). 'Acute myeloid leukemia: a comprehensive review and 2016 update'. *Blood Cancer J.* 6, e441.
- de Lau, W., Peng, W.C., Gros, P., and Clevers, H. (2014). The R-spondin/Lgr5/Rnf43 module: regulator of Wnt signal strength. *Genes Dev.* 28, 305–316.
- Desterke, C., Petit, L., Sella, N., Chevallier, N., Cabeli, V., Coquelin, L., Durand, C., Oostendorp, R.A.J., Isambert, H., Jaffredo, T., and Charbord, P. (2020). Inferring gene networks in bone marrow hematopoietic stem cell-supporting stromal niche populations. *iScience* 23, 101222.
- Detmer, K., and Walker, A.N. (2002). Bone morphogenetic proteins act synergistically with haematopoietic cytokines in the differentiation of haematopoietic progenitors. *Cytokine* 17, 36–42.
- Dickson, G.J., Liberante, F.G., Kettyle, L.M., O'Hagan, K.A., Finnegan, D.P., Bullinger, L., Geerts, D., McMullin, M.F., Lappin, T.R., Mills, K.I., and Thompson, A. (2013). HOXA/PBX3 knockdown impairs growth and sensitizes cytogenetically normal acute myeloid leukemia cells to chemotherapy. *Haematologica* 98, 1216–1225.
- Döhner, H., Weisdorf, D.J., and Bloomfield, C.D. (2015). Acute myeloid leukemia. *N. Engl. J. Med.* 373, 1136–1152.
- Dupoux, A., Cartier, J., Cathelin, S., Filomenko, R., Solary, E., and Dubrez-Daloz, L. (2009). cIAP1-dependent TRAF2 degradation regulates the differentiation of monocytes into macrophages and their response to CD40 ligand. *Blood* 113, 175–185.
- Ebinger, S., Zeller, C., Carlet, M., Senft, D., Bagnoli, J.W., Liu, W.H., Rothenberg-Thurley, M., Enard, W., Metzeler, K.H., Herold, T., et al. (2020). Plasticity in growth behavior of patients' acute myeloid leukemia stem cells growing in mice. *Haematologica* 105, 2855–2860.
- Fuchs, O., Simakova, O., Klener, P., Cmejlova, J., Zivny, J., Zavadil, J., and Stopka, T. (2002). Inhibition of Smad5 in human hematopoietic progenitors blocks erythroid differentiation induced by BMP4. *Blood Cells Mol. Dis.* 28, 221–233.
- Funakoshi, K., Bagheri, M., Zhou, M., Suzuki, R., Abe, H., and Akashi, H. (2017). Highly sensitive and specific Alu-based quantification of human cells among rodent cells. *Sci. Rep.* 7, 13202.
- Gal, H., Amariglio, N., Trakhtenbrot, L., Jacob-Hirsh, J., Margalit, O., Avigdor, A., Nagler, A., Tavor, S., Ein-Dor, L., Lapidot, T., et al. (2006). Gene expression profiles of AML derived stem cells; similarity to hematopoietic stem cells. *Leukemia* 20, 2147–2154.
- Garg, S., Reyes-Palomares, A., He, L., Bergeron, A., Lavallée, V.P., Lemieux, S., Gendron, P., Rohde, C., Xia, J., Jagdhane, P., et al. (2019). Hepatic leukemia factor is a novel leukemic stem cell regulator in DNMT3A, NPM1, and FLT3-ITD triple-mutated AML. *Blood* 134, 263–276.
- Genthe, J.R., and Clements, W.K. (2017). R-spondin 1 is required for specification of hematopoietic stem cells through Wnt16 and Vegfa signaling pathways. *Development* 144, 590–600.
- Glinka, A., Wu, W., Delius, H., Monaghan, A.P., Blumenstock, C., and Niehrs, C. (1998). Dickkopf-1 is a member of a new family of secreted proteins and functions in head induction. *Nature* 391, 357–362.
- Glinka, A., Dolde, C., Kirsch, N., Huang, Y.L., Kazanskaya, O., Ingelfinger, D., Boutros, M., Cruciati, C.M., and Niehrs, C. (2011). LGR4 and LGR5 are R-spondin receptors mediating Wnt/beta-catenin and Wnt/PCP signalling. *EMBO Rep.* 12, 1055–1061.
- Goldman, M., Craft, B., Hastie, M., Repecka, K., Kamath, A., McDade, F., Rogers, D., Brooks, A., Zhu, J., and Haussler, D. (2019). The UCSC Xena platform for public and private cancer genomics data visualization and interpretation. *bioRxiv*, 326470.
- Golub, T.R., Slonim, D.K., Tamayo, P., Huard, C., Gaasenbeek, M., Mesirov, J.P., Coller, H., Loh, M.L., Downing, J.R., Caligiuri, M.A., et al. (1999). Molecular classification of cancer: class discovery and class prediction by gene expression monitoring. *Science* 286, 531–537.
- Gruber, T.A., Larson Gedman, A., Zhang, J., Koss, C.S., Marada, S., Ta, H.Q., Chen, S.C., Su, X., Ogden, S.K., Dang, J., et al. (2012). An Inv(16)(p13.3q24.3)-encoded CBFA2T3-GLIS2 fusion protein defines an aggressive subtype of pediatric acute megakaryoblastic leukemia. *Cancer Cell* 22, 683–697.

- Hao, J., Ho, J.N., Lewis, J.A., Karim, K.A., Daniels, R.N., Gentry, P.R., Hopkins, C.R., Lindsley, C.W., and Hong, C.C. (2010). In vivo structure-activity relationship study of dorsomorphin analogues identifies selective VEGF and BMP inhibitors. *ACS Chem. Biol.* 5, 245–253.
- Hao, H.X., Xie, Y., Zhang, Y., Charlat, O., Oster, E., Avello, M., Lei, H., Mickanin, C., Liu, D., Ruffner, H., et al. (2012). ZNRF3 promotes Wnt receptor turnover in an R-spondin-sensitive manner. *Nature* 485, 195–200.
- Hao, H.X., Jiang, X., and Cong, F. (2016). Control of Wnt Receptor Turnover by R-spondin-ZNRF3/RNF43 Signaling Module and Its Dysregulation in Cancer. *Cancers (Basel)* 8, 54.
- Heldin, C.H., and Moustakas, A. (2016). Signaling receptors for TGF-beta family members. *Cold Spring Harb. Perspect. Biol.* 8, a022053.
- Heldin, C.H., Miyazono, K., and ten Dijke, P. (1997). TGF-beta signalling from cell membrane to nucleus through SMAD proteins. *Nature* 390, 465–471.
- Huang, S.M., Mishina, Y.M., Liu, S., Cheung, A., Stegmeier, F., Michaud, G.A., Charlat, O., Willellette, E., Zhang, Y., Wiessner, S., et al. (2009). Tankyrase inhibition stabilizes axin and antagonizes Wnt signalling. *Nature* 461, 614–620.
- Ilmer, M., Boiles, A.R., Regel, I., Yokoi, K., Michalski, C.W., Wistuba, I.I., Rodriguez, J., Alt, E., and Vykoukal, J. (2015). RSPO2 enhances canonical Wnt signaling to confer stemness-associated traits to susceptible pancreatic cancer cells. *Cancer Res.* 75, 1883–1896.
- Imai, Y., Kurokawa, M., Izutsu, K., Hangaishi, A., Maki, K., Ogawa, S., Chiba, S., Mitani, K., and Hirai, H. (2001). Mutations of the Smad4 gene in acute myelogenous leukemia and their functional implications in leukemogenesis. *Oncogene* 20, 88–96.
- Ivey, A., Hills, R.K., Simpson, M.A., Jovanovic, J.V., Gilkes, A., Grech, A., Patel, Y., Bhudia, N., Farah, H., Mason, J., et al.; UK National Cancer Research Institute AML Working Group (2016). Assessment of minimal residual disease in standard-risk AML. *N. Engl. J. Med.* 374, 422–433.
- Jiang, Y., Liang, H., Guo, W., Kottickal, L.V., and Nagarajan, L. (2000). Differential expression of a novel C-terminally truncated splice form of SMAD5 in hematopoietic stem cells and leukemia. *Blood* 95, 3945–3950.
- Kazanskaya, O., Glinka, A., del Barco Barrantes, I., Stanek, P., Niehrs, C., and Wu, W. (2004). R-Spondin2 is a secreted activator of Wnt/beta-catenin signaling and is required for *Xenopus* myogenesis. *Dev. Cell* 7, 525–534.
- Kim, K.A., Kakitani, M., Zhao, J., Oshima, T., Tang, T., Binnerts, M., Liu, Y., Boyle, B., Park, E., Emtage, P., et al. (2005). Mitogenic influence of human R-spondin1 on the intestinal epithelium. *Science* 309, 1256–1259.
- Klauzinska, M., Baljinnyam, B., Raafat, A., Rodriguez-Canales, J., Strizzi, L., Greer, Y.E., Rubin, J.S., and Callahan, R. (2012). Rspo2/Int7 regulates invasiveness and tumorigenic properties of mammary epithelial cells. *J. Cell. Physiol.* 227, 1960–1971.
- Konopleva, M.Y., and Jordan, C.T. (2011). Leukemia stem cells and microenvironment: biology and therapeutic targeting. *J. Clin. Oncol.* 29, 591–599.
- Koo, B.K., Spit, M., Jordens, I., Low, T.Y., Stange, D.E., van de Wetering, M., van Es, J.H., Mohammed, S., Heck, A.J., Maurice, M.M., and Clevers, H. (2012). Tumour suppressor RNF43 is a stem-cell E3 ligase that induces endocytosis of Wnt receptors. *Nature* 488, 665–669.
- Lee, H., Seidl, C., Sun, R., Glinka, A., and Niehrs, C. (2020). R-spondins are BMP receptor antagonists in *Xenopus* early embryonic development. *Nat. Commun.* 11, 5570.
- Li, S., Garrett-Bakelman, F.E., Chung, S.S., Sanders, M.A., Hricik, T., Rapaport, F., Patel, J., Dillon, R., Vijay, P., Brown, A.L., et al. (2016). Distinct evolution and dynamics of epigenetic and genetic heterogeneity in acute myeloid leukemia. *Nat. Med.* 22, 792–799.
- Liu, B., Sun, Y., Jiang, F., Zhang, S., Wu, Y., Lan, Y., Yang, X., and Mao, N. (2003). Disruption of Smad5 gene leads to enhanced proliferation of high-proliferative potential precursors during embryonic hematopoiesis. *Blood* 101, 124–133.
- Lugthart, S., van Drunen, E., van Norden, Y., van Hoven, A., Erpelinck, C.A., Valk, P.J., Beverloo, H.B., Löwenberg, B., and Delwel, R. (2008). High EVI1 levels predict adverse outcome in acute myeloid leukemia: prevalence of EVI1 overexpression and chromosome 3q26 abnormalities underestimated. *Blood* 111, 4329–4337.
- Majeti, R., Becker, M.W., Tian, Q., Lee, T.L., Yan, X., Liu, R., Chiang, J.H., Hood, L., Clarke, M.F., and Weissman, I.L. (2009). Dysregulated gene expression networks in human acute myelogenous leukemia stem cells. *Proc. Natl. Acad. Sci. USA* 106, 3396–3401.
- Massagué, J. (1998). TGF-beta signal transduction. *Annu. Rev. Biochem.* 67, 753–791.
- Nanki, K., Toshimitsu, K., Takano, A., Fujii, M., Shimokawa, M., Ohta, Y., Matano, M., Seino, T., Nishikori, S., Ishikawa, K., et al. (2018). Divergent routes toward Wnt and R-spondin niche independency during human gastric carcinogenesis. *Cell* 174, 856–869.e17.
- Nowak, D., Stewart, D., and Koeffler, H.P. (2009). Differentiation therapy of leukemia: 3 decades of development. *Blood* 113, 3655–3665.
- Pardali, E., Makowski, L.M., Leffers, M., Borgschieper, A., and Waltenberger, J. (2018). BMP-2 induces human mononuclear cell chemotaxis and adhesion and modulates monocyte-to-macrophage differentiation. *J. Cell. Mol. Med.* 22, 5429–5438.
- Raymond, A., Liu, B., Liang, H., Wei, C., Guindani, M., Lu, Y., Liang, S., St John, L.S., Molldrem, J., and Nagarajan, L. (2014). A role for BMP-induced homeobox gene MIXL1 in acute myelogenous leukemia and identification of type I BMP receptor as a potential target for therapy. *Oncotarget* 5, 12675–12693.
- Rocher, C., Singla, R., Singal, P.K., Parthasarathy, S., and Singla, D.K. (2012). Bone morphogenetic protein 7 polarizes THP-1 cells into M2 macrophages. *Can. J. Physiol. Pharmacol.* 90, 947–951.
- Salik, B., Yi, H., Hassan, N., Santiapillai, N., Vick, B., Connerty, P., Duly, A., Trahair, T., Woo, A.J., Beck, D., et al. (2020). Targeting RSPO3-LGR4 Signaling for Leukemia Stem Cell Eradication in Acute Myeloid Leukemia. *Cancer Cell* 38, 263–278.e6.
- Seshagiri, S., Stawiski, E.W., Durinck, S., Modrusan, Z., Storm, E.E., Conboy, C.B., Chaudhuri, S., Guan, Y., Janakiraman, V., Jaiswal, B.S., et al. (2012). Recurrent R-spondin fusions in colon cancer. *Nature* 488, 660–664.
- Shao, Y., Chen, Q.Z., Zeng, Y.H., Li, Y., Ren, W.Y., Zhou, L.Y., Liu, R.X., Wu, K., Yang, J.Q., Deng, Z.L., et al. (2016). All-trans retinoic acid shifts rosiglitazone-induced adipogenic differentiation to osteogenic differentiation in mouse embryonic fibroblasts. *Int. J. Mol. Med.* 38, 1693–1702.
- Szenker-Ravi, E., Altunoglu, U., Leushacke, M., Bosso-Lefèvre, C., Khatoor, M., Thi Tran, H., Naert, T., Noelanders, R., Hajamohideen, A., Beneteau, C., et al. (2018). RSPO2 inhibition of RNF43 and ZNRF3 governs limb development independently of LGR4/5/6. *Nature* 557, 564–569.
- Topić, I., Ikić, M., Ivčević, S., Kovačić, N., Marušić, A., Kušec, R., and Grčević, D. (2013). Bone morphogenetic proteins regulate differentiation of human promyelocytic leukemia cells. *Leuk. Res.* 37, 705–712.
- Tyner, J.W., Tognon, C.E., Bottomly, D., Wilmot, B., Kurtz, S.E., Savage, S.L., Long, N., Schultz, A.R., Traer, E., Abel, M., et al. (2018). Functional genomic landscape of acute myeloid leukaemia. *Nature* 562, 526–531.
- Voeltzel, T., Flores-Violante, M., Zylbersztejn, F., Lefort, S., Billandon, M., Jeanpierre, S., Joly, S., Fossard, G., Milenkovic, M., Mazurier, F., et al. (2018). A new signaling cascade linking BMP4, BMPR1A, ΔNp73 and NANOG impacts on stem-like human cell properties and patient outcome. *Cell Death Dis.* 9, 1011.
- Wang, S., and Chen, Y.G. (2018). BMP signaling in homeostasis, transformation and inflammatory response of intestinal epithelium. *Sci. China Life Sci.* 61, 800–807.
- Wang, N., Kim, H.G., Cotta, C.V., Wan, M., Tang, Y., Klug, C.A., and Cao, X. (2006). TGFbeta/BMP inhibits the bone marrow transformation capability of Hoxa9 by repressing its DNA-binding ability. *EMBO J.* 25, 1469–1480.
- Wang, Y., Krivtsov, A.V., Sinha, A.U., North, T.E., Goessling, W., Feng, Z., Zon, L.I., and Armstrong, S.A. (2010). The Wnt/beta-catenin pathway is required for the development of leukemia stem cells in AML. *Science* 327, 1650–1653.
- Wang, Y., Gao, J., Wang, H., Wang, M., Wen, Y., Guo, J., Su, P., Shi, L., Zhou, W., and Zhou, J. (2019). R-spondin2 promotes hematopoietic differentiation of

- human pluripotent stem cells by activating TGF beta signaling. *Stem Cell Res. Ther.* **10**, 136.
- Weinstein, J.N., Collisson, E.A., Mills, G.B., Shaw, K.R., Ozenberger, B.A., Ellrott, K., Shmulevich, I., Sander, C., and Stuart, J.M. (2013). The Cancer Genome Atlas Pan-Cancer analysis project. *Nature genetics* **45**, 1113–1120.
- Wiederschain, D., Wee, S., Chen, L., Loo, A., Yang, G., Huang, A., Chen, Y., Caponigro, G., Yao, Y.M., Lengauer, C., et al. (2009). Single-vector inducible lentiviral RNAi system for oncology target validation. *Cell Cycle* **8**, 498–504.
- Wu, C., Qiu, S., Lu, L., Zou, J., Li, W.F., Wang, O., Zhao, H., Wang, H., Tang, J., Chen, L., et al. (2014). RSPO2-LGR5 signaling has tumour-suppressive activity in colorectal cancer. *Nat. Commun.* **5**, 3149.
- Yang, S., Kim, C.Y., Hwang, S., Kim, E., Kim, H., Shim, H., and Lee, I. (2017). COEXPEDIA: exploring biomedical hypotheses via co-expressions associated with medical subject headings (MeSH). *Nucleic Acids Res.* **45** (D1), D389–D396.
- Yeung, J., Esposito, M.T., Gandillet, A., Zeisig, B.B., Griessinger, E., Bonnet, D., and So, C.W. (2010). β -Catenin mediates the establishment and drug resistance of MLL leukemic stem cells. *Cancer Cell* **18**, 606–618.
- Zangenberg, M., Grubach, L., Aggerholm, A., Silkjaer, T., Juhl-Christensen, C., Nyvold, C.G., Kjeldsen, E., Ommen, H.B., and Hokland, P. (2009). The combined expression of HOXA4 and MEIS1 is an independent prognostic factor in patients with AML. *Eur. J. Haematol.* **83**, 439–448.
- Zhang, H., Han, X., Wei, B., Fang, J., Hou, X., Lan, T., and Wei, H. (2019). RSPO2 enhances cell invasion and migration via the WNT/ β -catenin pathway in human gastric cancer. *J. Cell. Biochem.* **120**, 5813–5824.
- Zhu, Y.M., Wang, P.P., Huang, J.Y., Chen, Y.S., Chen, B., Dai, Y.J., Yan, H., Hu, Y., Cheng, W.Y., Ma, T.T., et al. (2017). Gene mutational pattern and expression level in 560 acute myeloid leukemia patients and their clinical relevance. *J. Transl. Med.* **15**, 178.

STAR★METHODS

KEY RESOURCES TABLE

REAGENT or RESOURCE	SOURCE	IDENTIFIER
Antibodies		
Rabbit monoclonal anti-Phospho-Smad1/5	Cell Signaling Technology	Cat#9516; RRID: AB_491015
Rabbit polyclonal anti-Smad1	Cell Signaling Technology	Cat#9743; RRID: AB_2107780
Mouse monoclonal anti-Smad1	Cell Signaling Technology	Cat#SC7965; RRID: AB_628261
Rabbit monoclonal anti-Axin1	Cell Signaling Technology	Cat#2074; RRID: AB_2062419
Mouse monoclonal anti-beta Catenin	BD Biosciences	Cat#610154; RRID: AB_397555
Mouse monoclonal anti-alpha-Tubulin	Sigma-Aldrich	Cat#T5168; RRID: AB_477579
Rabbit polyclonal anti-Erk1/2	Sigma-Aldrich	Cat#: M8159; RRID:AB_477245
Goat polyclonal anti-Human R-Spondin 2	R and D Systems	Cat#AF3266; RRID: AB_2285296
Mouse monoclonal anti-CD14	BD Biosciences	Cat#555396; RRID: AB_395797
Rat monoclonal anti-CD11B	BD Biosciences	Cat#557394; RRID: AB_396677
Rabbit monoclonal anti-Caspase-3	BD Biosciences	Cat#559565; RRID: AB_397274
Mouse monoclonal anti-CD14	BD Biosciences	Cat#561712; RRID: AB_10893199
Rat monoclonal anti-CD11B	BD Biosciences	Cat#557396; RRID: AB_396679
Mouse monoclonal anti-BrdU	BD Biosciences	Cat#347580; RRID: AB_10015219
Anti-human CD34-APC	BD biosciences	Cat# 555824; RRID:AB_398614
Anti-human CD45RA-PE	BD bioscience	Cat# 555489; RRID:AB_395880
Anti-human CD11b-PECy5	Biolegend	Cat# 301308; RRID:AB_314160
Anti-human CD14-APC-Cy7	Biolegend	Cat# 325620; RRID:AB_830693
F4/80 Monoclonal Antibody (BM8), APC	Thermo Fisher	Cat# 17-4801-80; RRID:AB_2784647
Mouse monoclonal anti-CD45	BD Biosciences	Cat#560973; RRID: AB_10565969
Goat polyclonal anti-GFP	Antibodies-Online	Cat#ABIN100085; RRID: AB_10778192
Mouse monoclonal IgG1-kappa, APC conjugated	BD Biosciences	Cat#550854; RRID: AB_398467
Mouse monoclonal IgG2a, FITC conjugated	BD Biosciences	Cat#556652; RRID: AB_479607
Rat monoclonal IgG2b, FITC conjugated	BD Biosciences	Cat#556923; RRID: AB_479623
Donkey polyclonal Anti-Rat IgG, Alexa Fluor 488	Invitrogen	Cat#A21208; RRID: AB_2535794
Goat polyclonal Anti-Mouse IgG, Alexa Fluor 488	Invitrogen	Cat#A11029; RRID: AB_2534088
Bacterial and virus strains		
Lentivirus	3rd Generation	N/A
Biological samples		
THP-1 xenograft NSG mice blood	This paper	N/A
THP-1 xenograft NSG mice bone marrow	This paper	N/A
THP-1 xenograft NSG mice liver	This paper	N/A
THP-1 xenograft NSG mice spleen	This paper	N/A
THP-1 xenograft NSG mice	This paper	N/A
Patient-derived xenografts (PDX), AML-661	University Hospital Heidelberg	N/A
Cord blood CD34 cells	Department of Obstetrics at University Hospital Heidelberg	N/A
Mouse bone marrow cells	C57BL/6N mice	N/A
Buffy coat	Blood bank of University Hospital Heidelberg	N/A

(Continued on next page)

Continued

REAGENT or RESOURCE	SOURCE	IDENTIFIER
Chemicals, peptides, and recombinant proteins		
DharmaFECT 1 transfection reagent	Dharmacon	CAT#T-2001
Lipofectamine RNAiMAX	Invitrogen	CAT#13778030
X-tremeGENE9 DNA transfection reagent	Roche	CAT#06365809001
Recombinant human BMP4 protein	R and D systems	CAT#314-BP
Recombinant human RSPO2 protein	R and D systems	CAT#3266-RS
Fc Receptor Binding Inhibitor	eBioscience	CAT#14916173
LDN 193185	Tocris	CAT#6053
DMH2	Sigma-Aldrich	CAT#SML1535
ACK Lysing Buffer	GIBCO	CAT#A1049201
SuperSignal West pico ECL	ThermoFisher	CAT#34580
Clarity Western ECL	Biorad	CAT#1705061
Polybrene	Sigma-Aldrich	CAT#TR-1003
XAV-939	Selleckchem	CAT#S1180
Retinoic acid, ATRA	Sigma-Aldrich	CAT#R2625
Cytarabine, AraC	Selleckchem	CAT#S1648
Doxycycline	Sigma-Aldrich	CAT#D9891
Protamine sulfate	Sigma-Aldrich	CAT#P3369
BrdU	Sigma-Aldrich	CAT#B5002
cOMplete Protease Inhibitor Cocktail	Roche	CAT#11697498001
MethoCult H4034 Optimum	MethoCult	CAT#H4034
Murine M-CSF	Peprotech	CAT#315-02
Human M-CSF	Peprotech	CAT#300-25
Critical commercial assays		
Dual luciferase reporter assay system	Promega	CAT#E1960
Experimental models: Cell lines		
HEK293T	ATCC	CRL-3216 RRID:CVCL_0063
THP-1	gift from Dr. S.Wiemann, DKFZ, Heidelberg	N/A
THP-1 Tet-ON inducible shControl	This paper	N/A
THP-1 Tet-ON inducible shRSPO2 1	This paper	N/A
THP-1 Tet-ON inducible shRSPO2 2	This paper	N/A
HL60	gift from Dr. A. Trumpp, DKFZ, Heidelberg	N/A
MV4-11	gift from Dr. A. Trumpp, DKFZ, Heidelberg	N/A
MOLM13	gift from Dr. A. Trumpp, DKFZ, Heidelberg	N/A
MOLM14	gift from Dr. A. Trumpp, DKFZ, Heidelberg	N/A
NB4	gift from Dr. A. Trumpp, DKFZ, Heidelberg	N/A
U937	gift from Dr. A. Trumpp, DKFZ, Heidelberg	N/A
NOMO-1	gift from Dr. S. Fröhling, DKFZ, Heidelberg	N/A
L cells stably transfected with mouse WNT3A	ATCC	N/A
Control L cells (without stably transfected mouse Wnt3a)	ATCC	N/A
Experimental models: Organisms/strains		
NOD/SCID/IL2Rg null (NSG) mice	Center for Preclinical Research, DKFZ, Heidelberg	N/A
C57BL/6N mice	Center for Preclinical Research, DKFZ, Heidelberg	N/A
Oligonucleotides		
See Table S1 for oligonucleotides	N/A	N/A

(Continued on next page)

Continued

REAGENT or RESOURCE	SOURCE	IDENTIFIER
Recombinant DNA		
RSPO2 ^{ΔC/ΔFU1/ΔFU2} -flag-pCDNA3 (plasmids)	Kazanskaya et al., 2004; Lee et al., 2020	N/A
DKK-1-pCDNA3 (plasmid)	Glinka et al., 2011	N/A
Tet-pLKO-puro	Wiederschain et al., 2009	Addgene CAT#21915, RRID: Addgene_21915
pLKO-eGFP	Garg et al., 2019	N/A
Software and algorithms		
Fiji (ImageJ)	Fiji	https://fiji.sc/
GraphPad	Prism	https://www.graphpad.com:43
Photoshop CS6	Adobe	https://www.adobe.com/products/photoshop.html
LightCycler 480 software	Roche	https://www.lifescience.roche.com
LAS 3000 Reader ver 2.2	Fujifilm	https://www.fujifilm.com
FlowJo LLC	BD Biosciences	https://www.flowjo.com
FACSDiva software	BD Biosciences	https://www.bdbiosciences.com/en-us
Deposited data		
UCSC Xena database	Goldman et al., 2019	https://xena.ucsc.edu
GDC TCGA Acute Myeloid Leukemia dataset	Weinstein et al., 2013	https://portal.gdc.cancer.gov/projects/TCGA-LAML
BEAT AML	Tyner et al., 2018	http://www.vizome.org/aml/
TARGET AML	Bolouri et al., 2018	https://ocg.cancer.gov/programs/target/data-matrix
Leucegene AML	Canadian leucegene AML project	https://data.leucegene.irc.ca/overview
Corces et al. RNaseq data	Corces et al., 2016	GEO accession GSE74912

RESOURCE AVAILABILITY

Lead contact

Further information and requests for resources and reagents should be directed to and will be fulfilled by the Lead Contact, Christof Niehrs (niehrs@dkfz-heidelberg.de).

Materials availability

All unique/stable reagents generated in this study are available from the Lead Contact with a completed Materials Transfer Agreement.

Data and code availability

This paper analyzes existing and publicly available data, which are listed in the [Key resources table](#). This paper does not report original code. Any additional information required to reanalyze the data reported in this paper is available from the lead contact upon request.

EXPERIMENTAL MODEL AND SUBJECT DETAILS

Cell lines and growth conditions

HEK293T cells (ATCC) were maintained in DMEM High glucose (GIBCO 11960) supplemented with 10% FBS (Capricorn FBS-12A), 1% penicillin-streptomycin (Sigma P0781), and 2mM L-glutamine (Sigma G7513). THP-1, HL60, MV4-11, MOLM13, MOLM14, NB4, NOMO-1 and U937 cells were maintained in RPMI (GIBCO 21875) with 10% FBS, 1% penicillin-streptomycin, 2mM L-glutamine and 1mM sodium pyruvate (Sigma S8636). All cell lines were cultured at 37°C and 5% CO₂ in a humidity-controlled incubator. Mycoplasma contamination was negative in all cell lines used.

Primary cell culture

Human primary PDX AML cells ([Ebinger et al., 2020](#)) were originally derived from a 55-year-old female patient with AML. Cells were thawed and cultured in IMDM supplemented with 15% BIT (bovine serum albumin, insulin, transferrin, Stem Cell Technologies

09500), β -mercaptoethanol 10^{-4} M (GIBCO 21985023), Gentamicin 50 μ g/ml (Thermo 15750060), Ciprofloxacin 10 μ g/ml (Genhunter Q902), SCF 100 ng/ml (Shenandoah 100-04), FLT3L 50 ng/ml (Shenandoah 100-21), IL-3 20 ng/ml (Shenandoah 100-80) and G-CSF 20 ng/ml (Shenandoah 100-72).

Human cord blood samples were obtained from the umbilical cord of female newborn babies. Samples were collected after obtaining written informed consent at the Department of Obstetrics at University Hospital Heidelberg, following procedures that were approved by the Research Ethics Board of the Medical Faculty of Heidelberg University. CD34⁺ cells were isolated from fresh cord blood samples using Ficoll Hypaque (Thermo GE17-1440-02) density gradient and subjected to MACS microbeads (Miltenyi 130-100-453) selection. After purity check by cytometry, cells were cultured in IMDM supplemented with 20% BIT (Stem Cell Technologies 09500), β -mercaptoethanol 10^{-4} M (GIBCO 21985023), Gentamicin 50 μ g/ml (Thermo 15750060), Ciprofloxacin 10 μ g/ml (Genhunter Q902), SCF 100 ng/ml (Miltenyi 130-096-695), FLT3L 100 ng/ml (Miltenyi 130-096-479), TPO 50 ng/ml (Miltenyi 130-095-752), and UM171 35nM (Stem cell technologies 72912).

Mouse bone marrow cells were flushed out with PBS from femurs of adult C57BL/6N mice. After removing red blood cells with ACK Lysis Buffer (GIBCO A1049201), cells were seeded into Petri dishes and maintained in DMEM High glucose supplemented with 10% FBS, 1% penicillin-streptomycin, 2mM L-glutamine and 1mM sodium pyruvate.

Human primary monocytes were isolated from buffy coats obtained from the blood bank of University Hospital Heidelberg, which were donated anonymously. After a gradient centrifugation with Ficoll-Paque (GE 17-5442-02), cells were seeded into Petri dishes for overnight incubation. Attached cells were washed with warm PBS and purity was checked by flow cytometry using CD14 antibodies. In all experiments, purity (% of CD14⁺ cells) was above 75 - 80%. Purified monocytes were maintained in RPMI supplemented with 10% FBS, 1% penicillin-streptomycin, 2mM L-glutamine and 1mM sodium pyruvate.

Animal experiments

NOD SCID gamma (NSG) mice were obtained from the Center for Preclinical Research, DKFZ, Heidelberg. Mice were maintained at a 12 h light-dark cycle with unrestricted Kliba 3307 diet and water. 7-8 weeks old female mice were used for this study. Mice were randomized for the cell injection. All mouse experiments were in accordance with the approved guidelines of the local Governmental Committee for Animal Experimentation (RP Karlsruhe, Germany, license G140/19).

METHOD DETAILS

siRNA transfection

siRNAs were transfected using DharmaFECT 1 transfection reagent (Dharmacon T-2001) or Lipofectamine RNAiMAX (Invitrogen, 13778030) according to the manufacturer protocols. Except otherwise mentioned, cells were harvested and analyzed 3 days after siRNA transfection. siRNA knockdown efficiencies were validated by qRT-PCR assay to be 60% reduction or greater.

Generation of conditioned medium

HEK293T cells were seeded in 15 cm culture dishes and transiently transfected with RSPO2-flag, or DKK1 plasmids using X-tremeGENE9 DNA transfection reagent (Roche 06365809001). After 24 hours, media were changed with fresh DMEM, 10% FBS, 1% L-glutamine and 1% penicillin-streptomycin and cultured 6 days at 32°C. Conditioned media were harvested three times every two days, centrifuged and validated by TOPflash assay or western blot analyses. WNT3A conditioned medium was produced in L-cells as previously described ([Kazanskaya et al., 2004](#)). RSPO2 deletion-variant media were generated and normalized as previously described ([Lee et al., 2020](#)).

TOPflash luciferase reporter assays

TOPflash luciferase assays were carried out as previously described ([Berger et al., 2017](#)). Briefly, HEK293T cells were seeded in a 96-well plate and transfected with 5 ng Topflash and 1 ng Renilla using X-tremeGENE9 DNA transfection reagent. Cells were overnight incubated as indicated and lysed for detection of luciferase activity using dual luciferase reporter assay system (Promega, E1960) according to the manufacturer protocols. Data are displayed as average of biological replicates with SD.

Western blot analysis

Cultured cells were harvested and lysed in cold RIPA buffer with cOmplete Protease Inhibitor Cocktail (Roche 11697498001). For analysis of cytosolic β -catenin, cells were extracted with saponin buffer ([Acebron et al., 2014](#)). Lysates were mixed with Laemmli buffer containing β -mercaptoethanol and boiled at 70°C for 10 min to prepare SDS-PAGE samples. Western blot images were acquired with SuperSignal West pico ECL (ThermoFisher 34580) or Clarity Western ECL (BioRad 1705061) using LAS-3000 system (FujiFilm). Quantification of blots was performed using ImageJ software.

Quantitative real-time PCR

Cultured cells were lysed in Macherey-Nagel RA1 buffer containing 1% β -mercaptoethanol and total RNAs were isolated using NucleoSpin RNA isolation kit (Macherey-Nagel 740955). Reverse transcription and PCR amplification were performed as described before ([Berger et al., 2017](#)). Briefly, 0.5-1.0 μ g RNA was reverse transcribed into cDNA and qPCR was done using a LightCycler

480 (Roche) and the indicated primers listed in [Key resources table](#). Graphs show relative gene expressions to GAPDH. Data are displayed as mean with SD from multiple experimental replicates. Statistical analyses were performed using PRISM7 software with unpaired t test or one-way ANOVA test.

FACS analysis

For analyzing macrophage differentiation of THP-1 and MOLM14, cells were harvested, pelleted and resuspended in ice-cold blocking buffer (PBS supplemented with 1% BSA and 0.1% NaN₃). Cells were treated with Fc Receptor Binding Inhibitor as recommended by the manufacturer (eBioscience 14916173) and stained directly with FITC/APC-conjugated antibodies diluted in blocking buffer or with non-conjugated primary antibodies followed by fluorochrome-labeled secondary antibodies. Isotype-matched antibodies were used as controls. Dead cells were excluded by counterstaining with propidium iodide. For analyzing apoptosis of THP-1, cells were fixed in 4% PFA, permeabilized by MeOH and blocked with PBS supplemented with 1% BSA and 0.1% Tween-20. Cells were stained with anti-active Caspase-3 antibody and fluorochrome-labeled secondary antibody. FACS Samples were analyzed with FACSCalibur or FACSCanto (BD Biosciences). 10,000 events per samples were acquired, and results were processed with Cell Quest, FACS-Diva software (BD Biosciences) or FlowJo. For BMP4 stimulation, cells were treated with 5 and 25 ng/ml recombinant human BMP4 protein (R&D systems 314-BP). 100, 300 and 1000 nM LDN 193185 (Tocris 6053) and 100, 300, 1,000 nM DMH2 (Sigma SML1535) were used for rescue assay. 1 or 10 nM of ATRA was used for THP-1 stimulation in relevant experiments. For the THP-1 cell number quantification and differentiation validation *in vivo*, bone marrow cells were harvested from femurs and tibias of NSG mice and red blood cells were removed by ACK Lysing Buffer. Cells were stained and analyzed as above. Human specific CD45 antibodies were used to distinguish THP-1 cells from mouse cells. Here, 50,000 PI-negative events per sample were acquired.

RSPO2 antibody neutralization assay

THP-1 cells were treated with 0.3, 1.0 and 3.0 µg/ml neutralizing goat polyclonal anti-RSPO2 antibodies (R&D systems AF3266) or goat polyclonal anti-GFP antibodies (ABIN 100085). After 48 hours, medium was replaced including fresh antibodies and incubated for another 24 hours. Western blot analysis and FACS analyses were performed as discussed above.

Generation of inducible shRNA expressing cell lines

The sequences of shRSPO2 and shControl ([Key resources table](#)) were synthesized, inserted into the transfer plasmid Tet-pLKO-puro and validated by sequencing. Tet-pLKO-puro was a gift from Dmitri Wiederschain (Addgene plasmid # 21915; <http://addgene.org/21915>; RRID: Addgene_21915). Lentivirus was produced with the 3rd generation lentiviral system according to the protocol available at the Trono lab as described (<https://www.epfl.ch/labs/tronolab/>). THP-1 and MOLM14 cells were infected with lentivirus with 8 µg/ml Polybrene (Sigma TR-1003) and selected with 0.5 µg/ml puromycin (Calbiochem 540411). Single cell clones were obtained by limiting dilutions. The shRNA expression of clones was validated by monitoring RSPO2 expression after doxycycline treatment (1.0 µg/ml) for 3 days. 1.0 µg/ml doxycycline was used for related experiments.

Cell cycle analysis with BrdU/PI double staining

Dox-inducible shRSPO2 RNA (TetOn-shRSPO2) THP-1 cells were incubated with 1.0 µg/ml Dox for 4 days. After 1 hr incubation with 10 µM BrdU, cells were harvested and fixed with ethanol. Following incubation with 2 N HCl/0.5% Triton X-100 and neutralization with 0.1 M sodium tetraborate (pH 8.5), cells were stained with anti-BrdU antibody (BD, clone B44) and corresponding FITC labeled secondary antibody. Finally, after incubation with RNase A and PI, cells were subjected to flow cytometry analysis.

Cytarabine/AraC IC₅₀ measurement and proliferation assay

Equal numbers of AML cells were treated with increasing concentrations of cytarabine (Selleck Chemicals) for 72 hours. The number of viable cells was counted with a TC20 Automated Cell Counter (BIO-RAD). Calculation of AraC IC₅₀ were performed using PRISM7 software. For measuring the IC₅₀ of THP-1 shRNA clones, cells were pretreated with doxycycline (1.0 µg/ml) for 2 days. For proliferation assay, equal numbers of cells were seed into cell culture dishes, and cell numbers were counted at the indicated days using a TC20 Automated Cell Counter (BIO-RAD). 1.0 µg/ml doxycycline and 1 and 3 µM of AraC were used in assays required.

Colony formation assay with THP-1 and MOLM14 cells

1,000 cells per well of Dox-inducible THP-1 and MOLM14 clones were seeded into 24-well plates in RPMI + 10% FBS, 1% penicillin-streptomycin, 1 mM sodium pyruvate, 2 mM L-glutamine and 0.5% methylcellulose, with or without Doxycycline (1 µg/ml). After 8 days incubation, microscopic dark field images were taken using LEICA DMIL microscope/Canon DS126311 camera. Quantification was executed with ImageJ, and statistics shows unpaired t test.

Lentivirus transduction of primary human cells and analysis

Lentivirus for primary cells was produced with pLKO-eGFP-shRNA as mentioned above. For transduction, primary human cells were incubated first with protamine sulfate for 30 min. Lentiviral particles were then added directly into culture media to give a multiplicity of infection (MOI) of 10-20. Gene transfer was checked via flow cytometry at 48-72h post infection. Cell sorting was performed on a BD FACS Aria II sorter against GFP. Flow cytometry data was acquired on a BD LSRII or Sartorius Intellicyt iQue3 flow cytometer

equipped with a High throughput sampler (HTS) device and analyzed using BD FACS Diva 4.0 or Flowjo softwares. Following antibodies were used for cell staining: CD34-APC (BD biosciences 555824), CD45RA-PE (BD bioscience 555489), CD11b-PECy5 (Biolegend 301308), CD14-APC-Cy7 (Biolegend 325620).

Colony formation assay with primary cord blood CD34⁺ cells

On day 4 post lentiviral transduction, 125 cord blood derived CD34⁺ cells were sorted into 0.5 mL methylcellulose (Methocult, Stem Cell Technologies 4034) supplied with gentamicin 50 µg/ml (Thermo 15750060) and plated in a 12-well format. After 10–14 days incubation, colonies were analyzed under an inverted microscope according their morphologies and statistics shows unpaired t test.

Mouse bone marrow cell analysis

Freshly isolated mouse bone marrow cells were transfected with siRNA and seeded into Ultra-Low Attachment plates (Corning CLS3471). 24 hours later, cells were treated with 20 ng/ml M-CSF (Peprotech, 315-02). After 3 additional days incubation, cells were harvested for flow cytometry, qRT-PCR and WB analysis. In case of LDN 193189 rescue assay, cells were co-treated with 100 nM LDN for 3 days before analysis.

Primary monocyte analysis

Freshly isolated human primary monocytes were transfected with siRNA and seeded into Ultra-Low Attachment plates. 48 hours later, cells were treated with 100 ng/ml M-CSF (Peprotech, 300-25). After 2 additional days incubation, cells were harvested for flow cytometry analysis (Dupoux et al., 2009). Samples for qRT-PCR analysis were harvested at 2 days after siRNA transfection.

Cytospin and Wright-Giemsa staining

Cells were harvested and washed in PBS, reaching final concentration of 25,000/100 µl. 100 µl cell suspension was centrifuged in a cytospin centrifuge (Shandon) for 5 min at 800 g. Wright-Giemsa staining was performed using a kit from ScyTek Laboratories.

In vivo THP-1 xenotransplantation into NSG mice and AML PDX experiments

For THP-1 xenotransplantation, randomized NSG mouse cohorts (n = 6–7 mice/group) were treated with Dox or vehicle throughout the study. Treatment started 3 days prior to cell transplantation via drinking water consisting 1 mg/ml Dox and 5% saccharose, or 5% saccharose only. One day prior to transplantation, mice were sub-lethally irradiated on whole body (2 Gy of a ¹³⁷Cs-source, Type OB. 58/9021; Buchler GmbH, Braunschweig) and treated with Baytril (25 mg/kg bodyweight, i. e. 25 mg/ml drinking water) for 2 weeks. 500,000 cells in 100 µl PBS were injected intravenously into the lateral tail vein of mice. Besides regular health checks, mouse body weight was taken twice per week throughout the experiment. Heparinized blood was collected from the tail vein at days 9 and 22 after transplantation. Terminal blood collection was performed under isoflurane anesthesia followed by cervical dislocation. Necropsies were taken as indicated or when mice reached a stop criterion described in the license, here defined as survival. For AML-661 PDX experiments, cells were overnight transduced with lentivirus and washed with PBS before tail vein injection. 250,000 cells per mouse were injected.

qPCR analysis for THP-1 burden in NSG mouse

Genomic DNA was isolated from mouse blood samples using NucleoSpin Tissue kit (Macherey-Nagel 740952). Quantitative PCR was done with human *Alu* element specific primers and corresponding Taqman probe (Funakoshi et al., 2017). For each reaction, 25 ng genomic DNA was used. A standard curve was generated with genomic DNA extracted from NSG mice blood containing known numbers of THP-1 cells and used for converting qPCR fluorescent signals to actual cell numbers. Normal NSG mice blood and nuclease free water were used as negative controls.

Expression analysis and Kaplan-Meier plot of patients with AML

Expression data and related clinical features were downloaded from the UCSC Xena database (<https://xena.ucsc.edu>) using GDC TCGA Acute Myeloid Leukemia cohort (<https://portal.gdc.cancer.gov/projects/TCGA-LAML>) and TARGET AML cohort (<https://ocg.cancer.gov/programs/target>), the BEAT AML website (<http://www.vizome.org/>) using the cohort from Tyner et al. (2018), the LeuceGene cohort (<https://leucegene.ca/>), and Corces et al. (2016). RNaseq data from different cohorts were generated with peripheral blood or bone marrow samples isolated from patients with AML and/or healthy individuals. Kaplan-Meier plots of patients with AML were generated with PRISM 7 and expression levels of indicated genes were stratified into two groups (high and low) based on the median of expression according to the RNaseq data.

QUANTIFICATION AND STATISTICAL ANALYSIS

Statistical analyses were done with the PRISM7 software using unpaired t test or one-way ANOVA followed by Tukey test. Log-rank test was used for survival analysis. Sample sizes and specific statistical test used are described in the Figure Legends. A significance threshold of $p \leq 0.05$ was used throughout the study. Not significant (ns), $p > 0.05$, * $p < 0.05$, ** $p < 0.01$, *** $p < 0.001$, **** $p < 0.0001$. Error bars indicate SD.

Cell Reports, Volume 36

Supplemental information

**RSPO2 inhibits BMP signaling to promote
self-renewal in acute myeloid leukemia**

Rui Sun, Lixiazi He, Hyeyoon Lee, Andrey Glinka, Carolin Andresen, Daniel Hübschmann, Irmela Jeremias, Karin Müller-Decker, Caroline Pabst, and Christof Niehrs

Supplementary Figure S1. RSP02 antagonizes BMP signalling in AML cells.

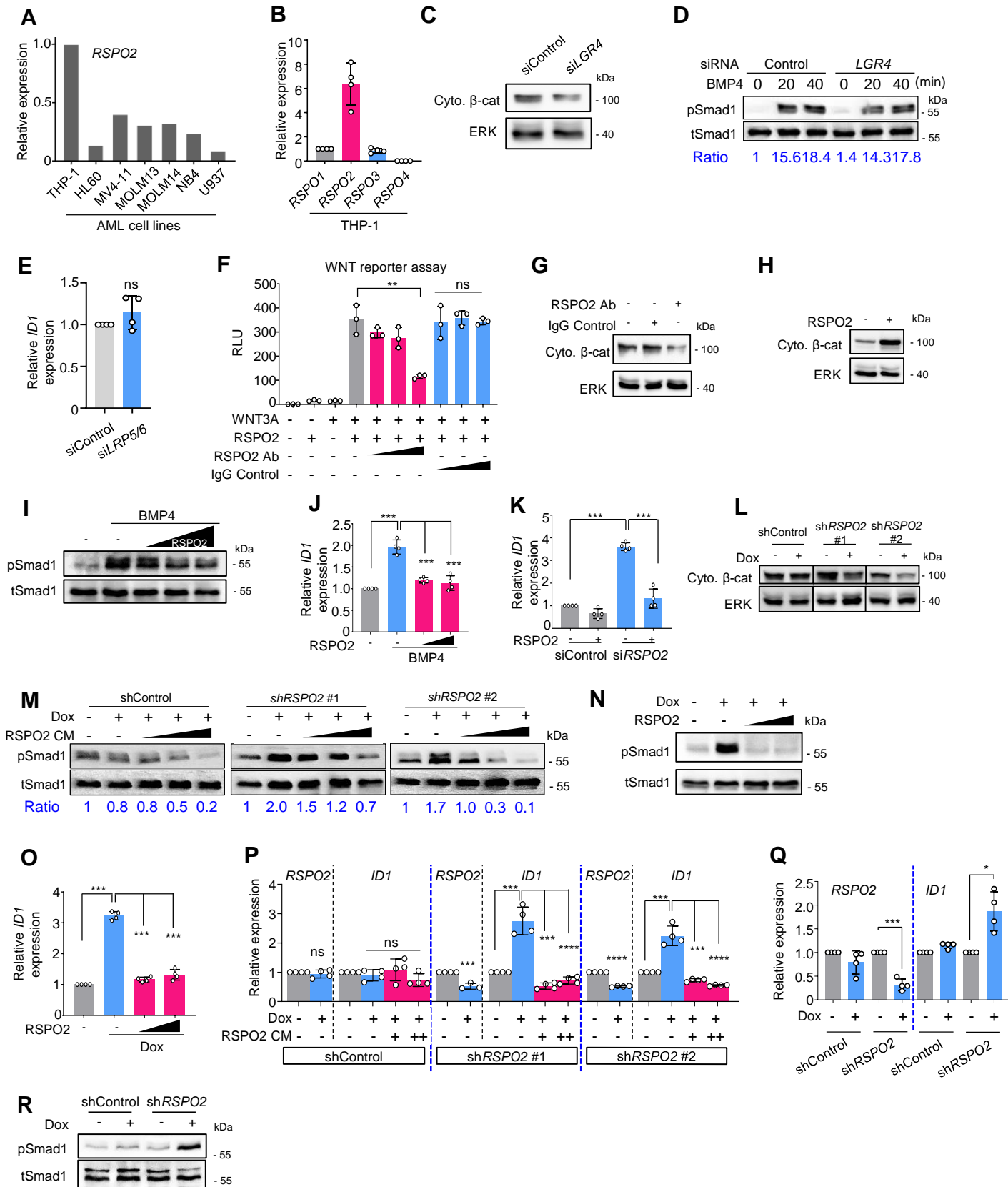


Figure S1: RSPO2 antagonizes BMP signalling in AML cells. Related to Figure 1.

(A) qRT-PCR analysis of *RSPO2* in AML cell lines. n = 1 per group.

(B) qRT-PCR analysis of *RSPO1-4* in THP-1 cells. n = 4 per group.

(C) Western blot analysis of cytosolic β -catenin in THP-1 cells upon si*LGR4* transfection.

(D) Western blot analysis of phosphorylated (p) Smad1 and total (t) Smad1 in THP-1 cells treated with siRNA and BMP4 as indicated. After overnight starvation, cells were stimulated with 5 ng/ml BMP4 for 20 and 40 min. Ratio shows relative levels of pSmad1 normalized to tSmad1. min, minute.

(E) qRT-PCR analysis of *ID1* in THP-1 cells treated with siRNA as indicated. n = 4 per group.

(F) TOPflash reporter assay in HEK293T cells treated with WNT3A, RSPO2 and antibody as indicated. After overnight incubation with WNT3A, RSPO2 and indicated antibodies, luciferase activity was measured. 0.3, 1.0 and 3.0 μ g/ml antibodies were used for the experiment. n = 3 per group. RLU, relative light units.

(G) Western blot analysis of cytosolic β -catenin in THP-1 cells upon antibody treatment as indicated. 3.0 μ g/ml antibodies were used for the experiment.

(H) Western blot analysis of cytosolic β -catenin in THP-1 cells upon treatment with RSPO2 recombinant protein (0.1 μ g/ml) for 24 hrs.

(I) Western blot analysis of phosphorylated (p) Smad1 and total (t) Smad1 in THP-1 cells treated with BMP4 and RSPO2 as indicated. After overnight starvation, cells were co-stimulated with 2.5 ng/mL BMP4 and increasing amount of RSPO2 (0.1, 0.2, 0.4 μ g/ml) for 30 min.

(J) qRT-PCR analysis of *ID1* in THP-1 cells treated with BMP4 (25 ng/ml) and RSPO2 (0.2, 0.4 μ g/ml). n = 4 per group.

(K) qRT-PCR analysis of *ID1* in THP-1 cells treated with siRNA and RSPO2 (0.2 μ g/ml) as indicated. n = 4 per group.

(L) Western blot analysis of cytosolic β -catenin in THP-1 shRNA clones after Dox treatment for 3 days.

(M) Western blot analysis of pSmad1 and tSmad1 in THP-1 clones treated as indicated. Cells were stimulated by Dox with or without increasing amount of RSPO2 conditional medium for 3 days.

(N) Western blot analysis of pSmad1 and tSmad1 in THP-1 sh*RSPO2* #1 cells treated as indicated. Cells were stimulated by Dox with or without increasing amount of RSPO2 recombinant protein (0.2, 0.5 μ g/ml) for 3 days.

(O) qRT-PCR analysis of *ID1* in THP-1 sh*RSPO2* #1 cells treated with as indicated. Cells were stimulated by Dox with or without increasing amount of RSPO2 recombinant protein (0.2, 0.5 μ g/ml) for 3 days. n = 4 per group.

(P) qRT-PCR analysis of *RSPO2* and *ID1* in THP-1 clones with Dox and RSPO2 treatment. Cells were stimulated by Dox with or without increasing amount of RSPO2 for 3 days. n = 4 per group.

(Q) qRT-PCR analysis of *RSPO2* and *ID1* in MOLM14 clones upon Dox treatment for 3 days. n = 4 per group.

(R) Western blot analysis of pSmad1 and tSmad1 in MOLM14 clones upon Dox treatment for 3 days. Results are presented as the mean \pm SD. *p < 0.05, **p < 0.01, ***p < 0.001, and ****p < 0.0001 from unpaired t-test for experiments with two groups or one-way ANOVA for experiments with more than two groups.

Supplementary Figure S2. RSPO2 inhibits differentiation of AML cells.

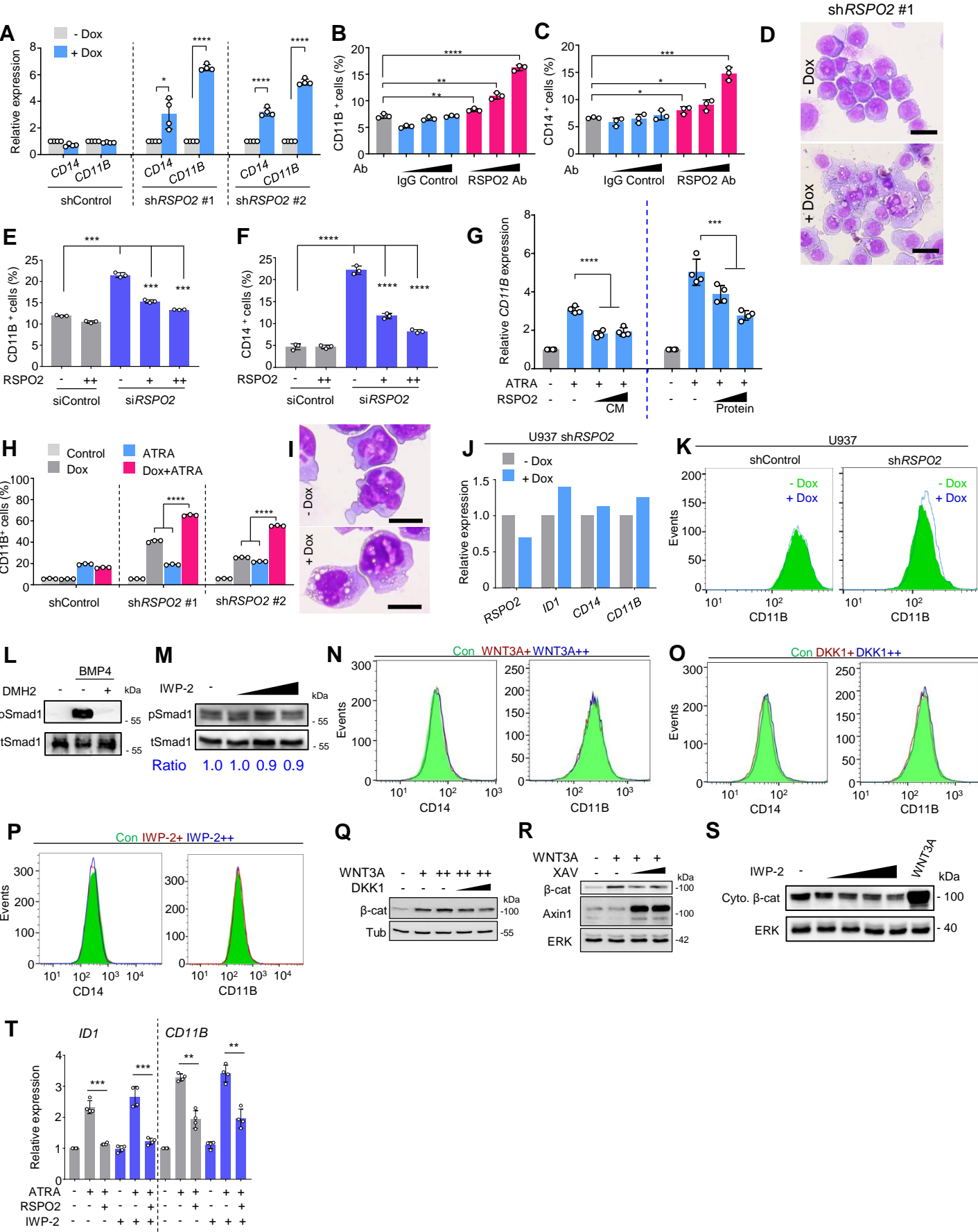


Figure S2. RSPO2 inhibits differentiation of AML cells. Related to **Figure 2**.

- (A) qRT-PCR analysis of *CD14* and *CD11B* in THP-1 clones upon Dox treatment for 3 days. n = 4 per group.
- (B-C) Quantification of FACS analysis for CD11B⁺- or CD14⁺ cells upon antibody treatment of THP-1 cells. 0.3, 1.0 and 3.0 µg/ml antibodies were used for the experiment. n = 3 per group.
- (D) Wright-Giemsa staining of THP-1 sh*RSPO2* #1 cells after Dox treatment for 8 days. Scale bar = 10 µM.
- (E-F) Quantification of FACS analysis for CD14⁺- or CD11B⁺ cells upon siRNA transfection and RSPO2 recombinant protein treatment. n = 3 per group.
- (G) qRT-PCR analysis of *CD11B* in THP-1 cells stimulated by 10 nM ATRA, with or without increasing amount of RSPO2 recombinant protein (0.2, 0.5 µg/ml) or conditioned medium for 3 days. n = 4 per group. ATRA, all-trans retinoic acid. CM, conditioned medium.
- (H) Quantification of FACS analysis for CD11B⁺ cells in THP-1 clones treated as indicated. Cells were stimulated by 1 nM ATRA and Dox for 3 days before analysis. n = 3 per group.
- (I) Wright-Giemsa staining of MOLM14 sh*RSPO2* cells after Dox treatment for 7 days. Scale bar = 10 µM.
- (J) qRT-PCR analysis for *RSPO2*, *ID1*, *CD14* and *CD11B* expression in U937 clone upon Dox treatment for 3 days. n=1 per group.
- (K) FACS analysis for CD11B⁺ cells in U937 clones upon Dox treatment for 3 days.
- (L) Western blot analysis of pSmad1 and tSmad1 in THP-1 cells after BMP4 and BMP receptor inhibitor DMH2 treatment. Cells were stimulated by 10 ng/ml BMP4 for 30 min. 100 nM DMH2 was added for another 30 min incubation before WB analysis.
- (M) Western blot analysis of pSmad1 and tSmad1 in THP-1 cells after overnight IWP-2 (1, 3 and 10 µM) treatment.
- (N-P) FACS plots for CD14⁺- or CD11B⁺ cells in THP-1 cells following overnight treatment with WNT3A (N), DKK1 (O), or IWP-2 (P).
- (Q-S) Western blot analyses in THP-1 cells treated as indicated. XAV, Axin stabilizer XAV 939. 0.01, 0.1, 1, 10 µM IWP-2 were used (S).
- (T) qRT-PCR analysis for *ID1* and *CD11B* expression in THP-1 cells treated as indicated. 10 µM ATRA, 0.01 µM IWP-2 and 0.4 µg/ml RSPO2 were used. n = 4 per group.

Results are presented as the mean ± SD. *p < 0.05, ***p < 0.001, and ****p < 0.0001 from unpaired t-test for experiments with two groups or one-way ANOVA for experiments with more than two groups.

Supplementary Figure S3. RSPO2 deficiency sensitizes THP-1 to chemotherapeutic drug treatment.

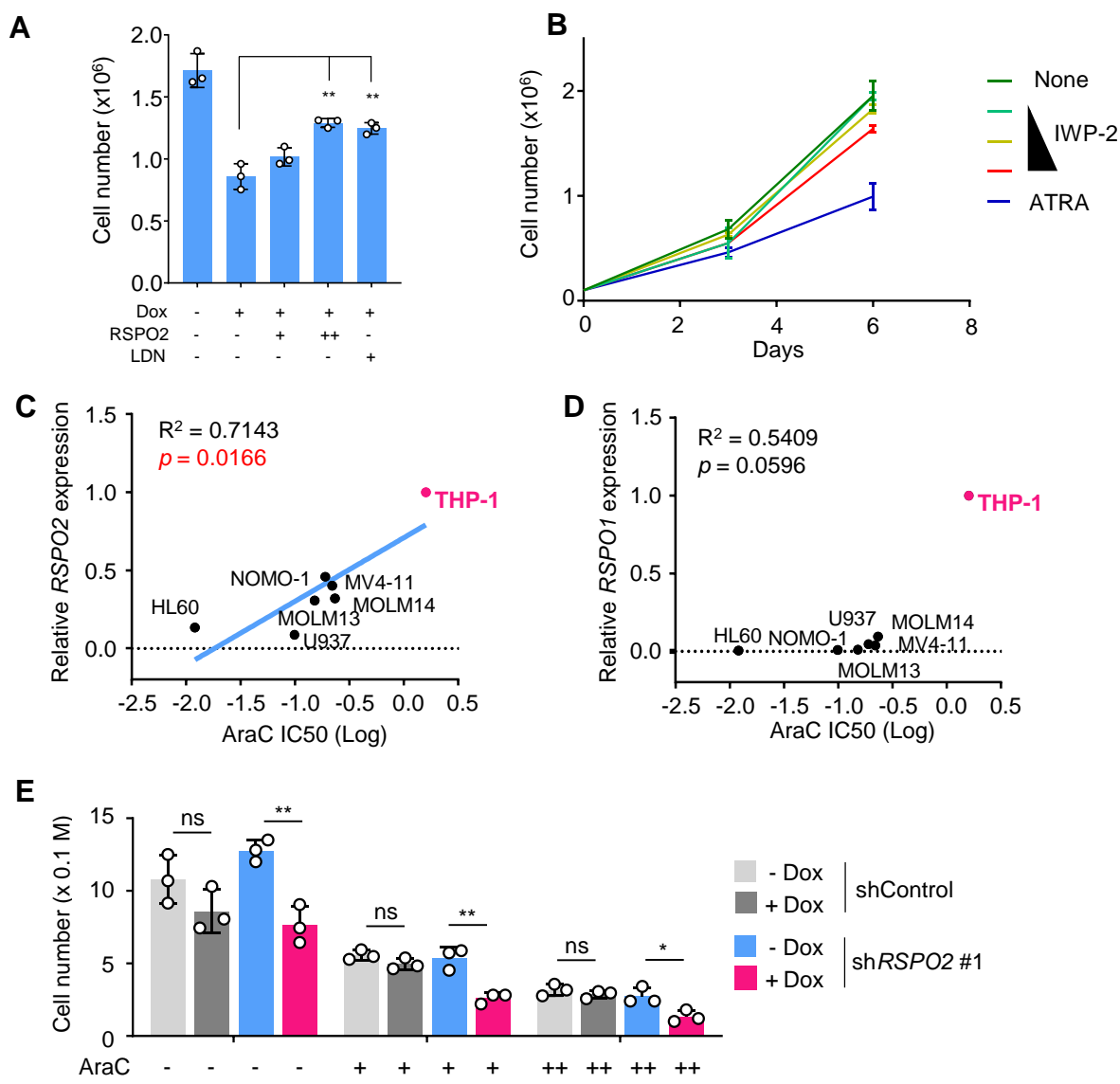


Figure S3. RSPO2 deficiency sensitizes THP-1 to chemotherapeutic drug treatment. Related to **Figure 3.**

(A) Total cell count of THP-1 shRSPO2 #1 cells treated with Dox, RSPO2 proteins (0.1, 0.2 µg/ml) and 200 nM LDN 193189 for 6 days. n = 3 per group.

(B) Total cell count of THP-1 cells treated with increasing amount of IWP-2 (1, 3, 10 µM) and 10 nM ATRA for 6 days. n = 3 per group.

(C-D) Correlation between the mRNA expression levels of *RSPO2/RSPO1* and AraC logIC₅₀ in different AML cell lines. IC₅₀ was determined after 3 days incubation with increasing amount of AraC.

(E) Total cell count of THP-1 clones treated with Dox and AraC at low (1 µM) or high dose (3 µM) for 3 days. n = 3 per group.

Results are presented as the mean ± SD. *p < 0.05, **p < 0.01 from unpaired t-test.

Supplementary Figure S4. Loss of *RSPO2* induces BMP signalling in primary blood cells.

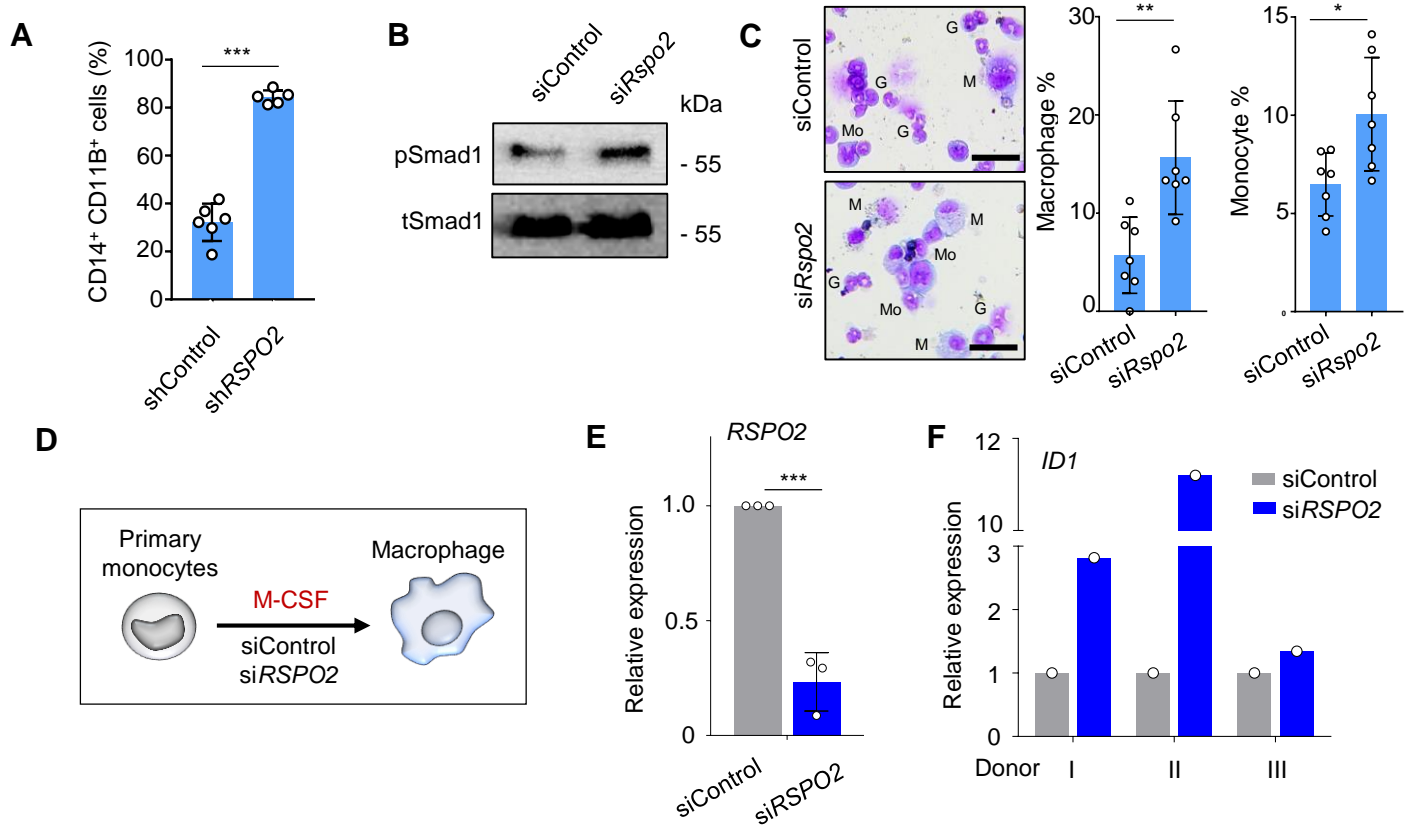


Figure S4. Loss of *RSPO2* induces BMP signalling in primary blood cells. Related to **Figure 4**.

(A) Quantification of FACS analysis on cells collected from colony formation assays (**Figure 4F**). n = 5/6 per group.

(B) Western blot analysis of phosphorylated (p) Smad1 and total (t) Smad1 in mouse bone marrow cells after siRNA transfection.

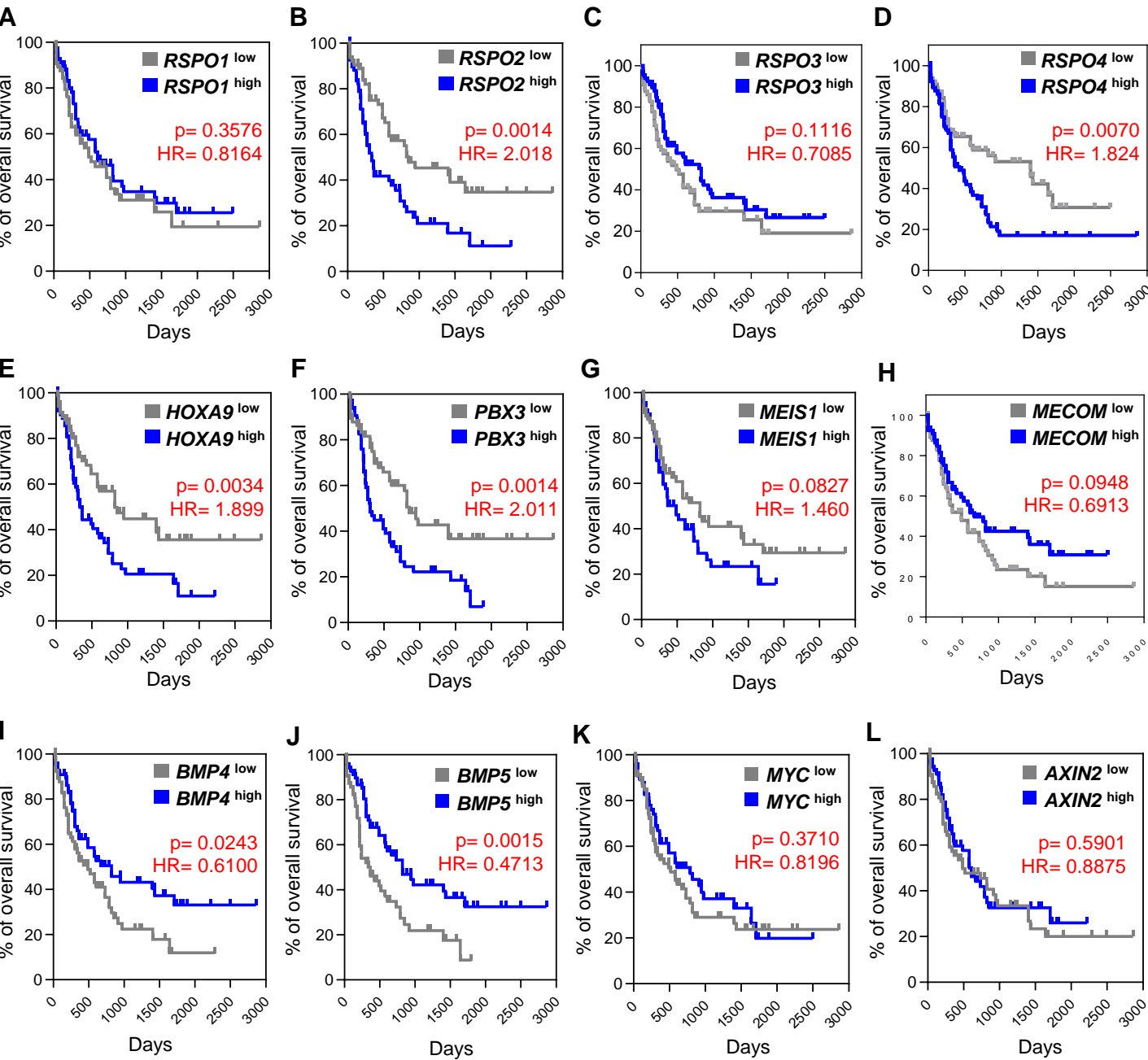
(C) Wright-Giemsa staining of mouse bone marrow cells upon siRNA transfection and M-CSF stimulation. Percentage of macrophages and monocytes was quantified from seven different fields based on the morphological characterization. Scale bar = 10 μ M. M, macrophage. Mo, monocyte. G, granulocyte.

(D) Scheme of experimental setup for human primary monocytes differentiation.

(E-F) qRT-PCR analysis for *RSPO2* and *ID1* expression in human primary monocytes upon siRNA transfection. (E), data pooled from three different donors. (F), data showing *ID1* expression in three different donors separately.

Results are presented as the mean \pm SD. *p < 0.05, **p < 0.01, ***p < 0.001 from unpaired t-test.

Supplementary Figure S5. High *RSPO2* expression is a predictor for poor prognosis in AML.



M Summary gene expression association with overall survival

GDC-TCGA AML	<i>RSPO1</i>	<i>RSPO2</i>	<i>RSPO3</i>	<i>RSPO4</i>	<i>HOXA9</i>	<i>PBX3</i>	<i>MEIS1</i>	<i>MECOM</i>	<i>BMP4</i>	<i>BMP5</i>	<i>MYC</i>	<i>AXIN2</i>
Low (n)	65	63	66	66	46	67	69	66	66	64	67	64
High (n)	67	69	66	66	43	65	63	66	66	68	65	68
Hazard ratio (HR)	0.8164	2.018	0.7085	1.824	1.899	2.011	1.460	0.6913	0.6100	0.5037	0.8196	0.8875
Median survival ratio	1.245	0.392	1.691	0.3026	0.408	0.3571	0.5912	1.372	1.681	2.246	1.529	1.243
Log-rank p	0.3576	0.0014	0.1116	0.0070	0.0034	0.0014	0.0827	0.0948	0.0243	0.0015	0.3710	0.5901
Significance	ns	**	ns	**	**	**	ns	ns	**	**	ns	ns

Figure S5. High *RSPO2* expression is a predictor for poor prognosis in AML. Related to **Figure 5**.

(A-L) Kaplan-Meier plot of AML patients stratified by different gene expression levels (low and high according to the median).

(M) Table showing the number of patients analyzed (n), hazard ratio (HR), median survival ratio and significance of survival differences. Log-rank test was used for statistical analysis.

Supplementary Figure S6. Loss of *RSPO2* reduces tumor burden in an AML xenograft model.

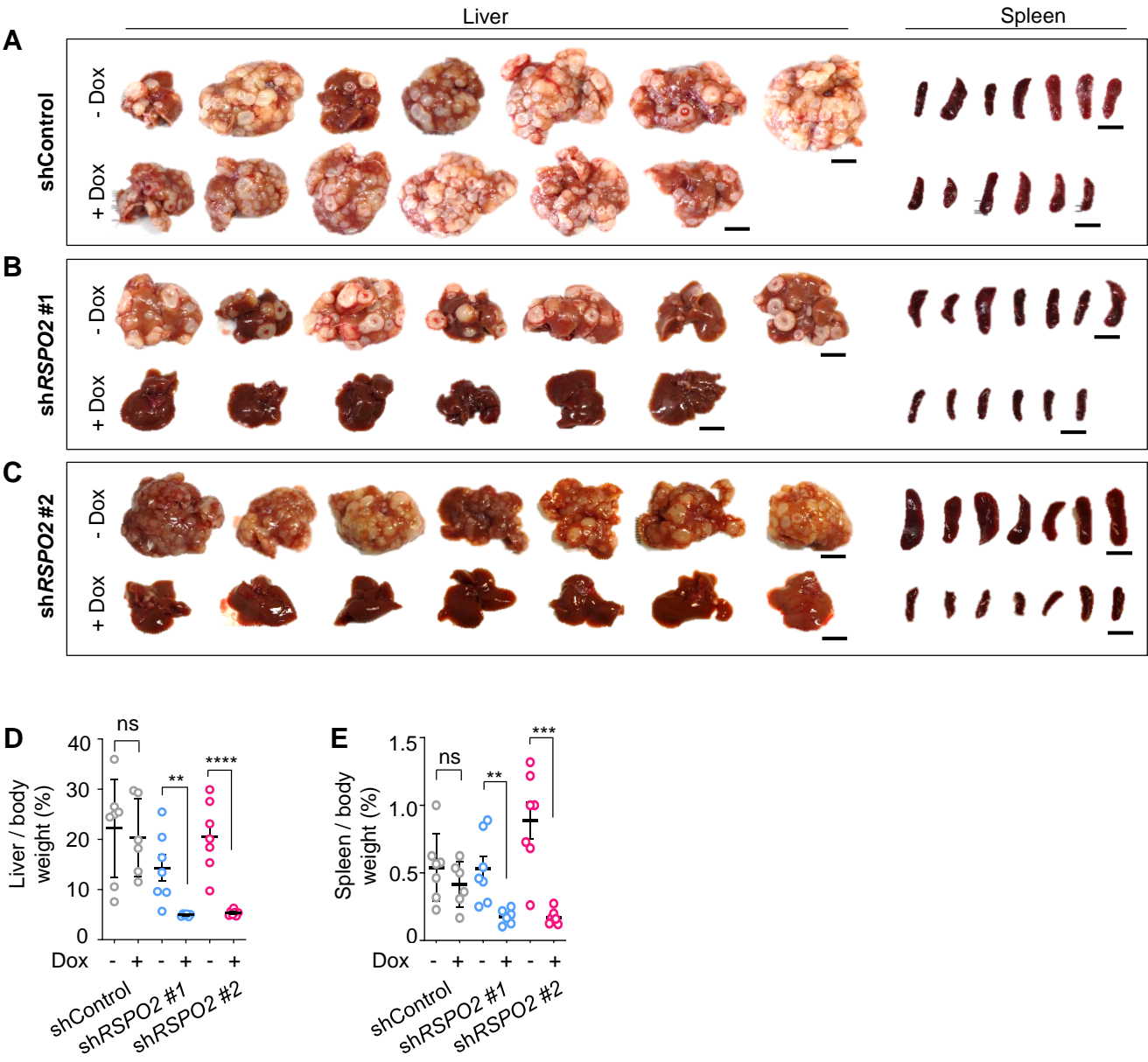


Figure S6. Loss of *RSPO2* reduces tumor burden in an AML xenograft model. Related to **Figure 6**.

(**A-C**) Images of livers and spleens harvested from mice xenografted with THP-1 cell lines expressing the indicated Dox-inducible shRNAs treated with (+) or without (-) Dox. Scale bar = 1 cm.

(**D-E**) Liver and spleen weights from mice xenografted with THP-1 cell lines expressing the indicated Dox-inducible shRNAs treated with (+) or without (-) Dox. Organ weights were normalized to total body weight of the corresponding mouse. Samples were analyzed on day 50 post cell-injection for shControl, day 57 post cell-injection for sh*RSPO2*-1 and day 42 post cell-injection for sh*RSPO2*-2 separately. Samples from Dox treated and not treated group were analyzed at the same time.

Results are presented as the mean \pm SD. ** $p < 0.01$, *** $p < 0.001$, **** $p < 0.0001$ from unpaired t-test.